

A convergent interacting particle method and computation of KPP front speeds in chaotic flows

Junlong Lyu^a, Zhongjian Wang^b, Jack Xin^c, Zhiwen Zhang^{a,*}

^a*Department of Mathematics, The University of Hong Kong, Pokfulam Road, Hong Kong SAR, China.*

^b*Department of Statistics, The University of Chicago, Chicago, IL 60637, USA.*

^c*Department of Mathematics, University of California at Irvine, Irvine, CA 92697, USA.*

Abstract

In this paper, we study the propagation speeds of reaction-diffusion-advection (RDA) fronts in time-periodic cellular and chaotic flows with Kolmogorov-Petrovsky-Piskunov (KPP) nonlinearity. We first apply the variational principle to reduce the computation of KPP front speeds to a principal eigenvalue problem of a linear advection-diffusion operator with space-time periodic coefficients on a periodic domain. To this end, we develop efficient Lagrangian particle methods to compute the principal eigenvalue through the Feynman-Kac formula. By estimating the convergence rate of Feynman-Kac semigroups and the operator splitting methods for approximating the linear advection-diffusion solution operators, we obtain convergence analysis for the proposed numerical methods. Finally, we present numerical results to demonstrate the accuracy and efficiency of the proposed method in computing KPP front speeds in time-periodic cellular and chaotic flows, especially the time-dependent Arnold-Beltrami-Childress (ABC) flow and time-dependent Kolmogorov flow in three-dimensional space.

AMS subject classification: 35K57, 47D08, 65C35, 65L20, 65N25.

Keywords: KPP front speeds; cellular and chaotic flows; Feynman-Kac semigroups; interacting particle method; operator splitting methods; eigenvalue problems; convergence analysis.

1. Introduction

Front propagation in complex fluid flows arises in many scientific areas such as chemical kinetics, combustion, biology, transport in porous media, and industrial deposition processes (see [46] for a review). A fundamental problem is to analyze and compute large-scale front speeds in complex flows. An extensively studied model problem is the reaction-diffusion-advection (RDA) equation with Kolmogorov-Petrovsky-Piskunov (KPP) nonlinearity [22]. To be specific, the KPP equation is

$$u_t = \kappa \Delta_{\mathbf{x}} u + (\mathbf{v} \cdot \nabla_{\mathbf{x}}) u + \tau^{-1} f(u), \quad t \in \mathbb{R}^+, \quad \mathbf{x} = (x_1, \dots, x_d)^T \in \mathbb{R}^d, \quad (1)$$

*Corresponding author

Email addresses: u3005480@connect.hku.hk (Junlong Lyu), zhongjian@statistics.uchicago.edu (Zhongjian Wang), jxin@math.uci.edu (Jack Xin), zhangzw@hku.hk (Zhiwen Zhang)

where κ is the diffusion constant, τ is the time scale of reaction rate, \mathbf{v} is an incompressible velocity field (its precise definition will be discussed later), u is the concentration of reactant or population, and the KPP reaction $f(u) = u(1-u)$ satisfying $f(u) \leq uf'(0)$. In our analysis and numerical examples, we will keep τ and κ fixed, while change the magnitude of the velocity field \mathbf{v} , which equivalently means changing the Péclet number.

Since the pioneering work of Kolmogorov, Petrovsky, and Piskunov [22] and Fisher [13] on traveling fronts of the reaction-diffusion equations, this field has gone through enormous growth and development. Reaction-diffusion front propagation in fluid flows has been an active research topic for decades; see e.g.[16, 44, 24, 45, 3, 32, 33, 46, 29] and references therein. Significant amounts of mathematical analysis and numerical works in this direction have been accomplished when the streamlines of fluid flow are either well-structured (regular motion) or fully random (ergodic motion). Yet, the often encountered less studied case is when the streamlines consist of both regular and irregular motions, while neither one takes up the entire phase space, such as the chaotic Arnold-Beltrami-Childress (ABC) flow [10, 4] and Kolmogorov flows [15, 7].

In recent years, much progress has been made in finite element computation of the KPP front propagation in time-periodic cellular and chaotic flows based on a linearized corrector equation. If the velocity field $\mathbf{v} = \mathbf{v}(\mathbf{x})$ in the KPP equation (1) is time-independent, the minimal front speed in direction \mathbf{e} is given by the variational formula [16]: $c^*(\mathbf{e}) = \inf_{\lambda > 0} \mu(\lambda)/\lambda$, where $\mu(\lambda)$ is the principal eigenvalue of the elliptic operator, \mathcal{A}_1^λ , namely,

$$\mathcal{A}_1^\lambda \Phi \equiv \kappa \Delta_{\mathbf{x}} \Phi + (2\lambda \mathbf{e} + \mathbf{v}) \cdot \nabla_{\mathbf{x}} \Phi + (\kappa \lambda^2 + \lambda \mathbf{v} \cdot \mathbf{e} + \tau^{-1} f'(0)) \Phi = \mu(\lambda) \Phi. \quad (2)$$

In Eq.(2), $\Phi \in L^2(\mathbb{T}^d)$, $\mathbb{T} = \mathbb{R}/\mathbb{Z}$ is the one-dimensional torus, and \mathbf{v} is period 1 in all direction $x_i, 1 \leq i \leq d$. Accurate estimation of $c^*(\mathbf{e})$ boils down to computing the principal eigenvalue of the operator \mathcal{A}_1^λ in (2). Adaptive finite element methods (FEM) were successfully applied to solve (2) in [40, 39]. If the velocity field $\mathbf{v} = \mathbf{v}(t, \mathbf{x})$ in the KPP equation (1) is periodic in time t , then the variational formula $c^*(\mathbf{e}) = \inf_{\lambda > 0} \mu(\lambda)/\lambda$ still holds [30], where $\mu(\lambda)$ is the principal eigenvalue [17] of the time-periodic parabolic operator, \mathcal{A}_2^λ , namely,

$$\mathcal{A}_2^\lambda \Phi \equiv \kappa \Delta_{\mathbf{x}} \Phi + (2\lambda \mathbf{e} + \mathbf{v}) \cdot \nabla_{\mathbf{x}} \Phi + (\kappa \lambda^2 + \lambda \mathbf{v} \cdot \mathbf{e} + \tau^{-1} f'(0)) \Phi - \Phi_t = \mu(\lambda) \Phi, \quad (3)$$

on the space-time domain $\mathbb{T}^d \times [0, T]$ (T is the period of \mathbf{v} in t), subject to the same boundary condition in \mathbf{x} as (1) and periodic in t . An edge-averaged FEM with algebraic multigrid acceleration was developed in [47] to study KPP front speeds in two-dimensional time-periodic cellular flows with chaotic streamlines. Adaptive FEM methods provide an efficient way to investigate the KPP front speeds in time-periodic cellular and chaotic flows. However, when the magnitude of velocity field is large and/or the dimension of spatial variables is big (e.g. $d = 3$), it is extremely expensive to compute KPP front speeds by using the FEM.

Recently, we have made significant progress in developing Lagrangian particle methods for computing effective diffusivities in chaotic and random flows [43, 42, 23]. This motivates us to develop interacting particle methods to compute KPP front propagation in time-periodic cellular and chaotic flows in this paper, especially in three-dimensional flows.

In this paper, we first apply operator splitting methods to approximate the solution operator of the linear advection-diffusion operator (see Eq.(4)), which is a non-autonomous evolution

equation and corresponding to the linearization of the KPP equation. Then, we develop Lagrangian numerical schemes to compute the KPP front propagation through the Feynman-Kac formula, which establishes a link between parabolic PDEs and SDEs. Direct approximation of the Feynman-Kac formula is unstable, since the main contribution to the expectation comes from sample paths that visit maximal points of the potential; see Eq.(7). Alternatively, we study a normalized version, i.e., the Feynman-Kac semigroup. Specifically, the principal eigenvalue of \mathcal{A}_1^λ and \mathcal{A}_2^λ can be obtained by studying the convergence of Feynman-Kac semigroups for SDEs associated with operators \mathcal{A}_1^λ and \mathcal{A}_2^λ [8, 12]. We approximate the evolution of probability measures by an interacting particle system and use the resampling technique to reduce the variance. Moreover, we estimate the approximation of semigroups associated with the solution operators of non-autonomous evolution equations and obtain convergence analysis for our method in computing the KPP front speeds.

We point out that using Feynman-Kac semigroups to estimate the principal eigenvalue of differential operators has a long history. It was developed in large deviation theory, where Feynman-Kac semigroups were used to calculate cumulant generating functions [9]. They were also used in important practical applications, such as the diffusion Monte Carlo (DMC) method [14]. In the case when the flow is autonomous, [12] gave a rigorous proof of convergence and error analysis using a backward error analysis approach. When the flow becomes non-autonomous, their method cannot be directly applied. There are several novelties in our paper. Firstly, we analyze the solution operator by an operator splitting method and estimate the error in the L_2 operator norm. Secondly, we prove the convergence of estimating principal eigenvalues by the Feynman-Kac semigroups for non-autonomous periodic systems. Furthermore, we develop the N -interacting particle system (N -IPS) method to calculate the principal eigenvalue, where several important 3D chaotic flows are investigated. Notice that when the magnitude of the velocity field is large and/or the dimension of spatial variables is three, it is extremely expensive to calculate the principal eigenvalue using the FEM and spectral method.

Finally, we carry out numerical experiments to demonstrate the accuracy and efficiency of the proposed method in computing KPP front speeds for time-periodic cellular and chaotic flows. Most importantly, we investigate the dependence of KPP front speeds on the chaos (disorder) and flow intensities. Let A denote the magnitude of the velocity field. For space-time-periodic shear flow, the speed $c^*(A)$ obeys a quadratic enhancement law: $c^*(A) = c_0(1 + \alpha A^2) + O(A^3)$, $A \ll 1$, where c_0 is the KPP front speed in homogeneous media ($A = 0$) and $\alpha > 0$ depends only on flow \mathbf{v} [31]. The study for complicated flows, e.g. 3D flows remains largely open. At large A , the solution of the principal eigenvalue problem (2) develops internal layers, which brings difficulties for the FEM and spectral method. We will study this issue in Section 4.3. Numerical results show that our interacting particle method is still very efficient when the magnitude of velocity field A is large and computational cost linearly depends on the dimension d of spatial variables in the KPP equation (1). Thus, we are able to compute the KPP front speeds for time-dependent cellular and chaotic flows of physical interests, including the ABC flows and the Kolmogorov flows in three-dimensional space. We numerically verify that the relationship between the KPP front speed $c^*(A)$ and the effective diffusivity $D^E(A)$, i.e. $c^*(A) = O(\sqrt{D^E(A)})$, is true in 2D steady cellular flows. To the best of our knowledge,

our work appears to be the first one in the literature to develop numerical methods to compute KPP front speeds in 3D time-dependent flows.

The rest of the paper is organized as follows. In Section 2, we propose Lagrangian interactive particle methods in computing KPP front speeds in time-periodic cellular and chaotic flows. In Section 3, we estimate the approximation of semigroups associated with the solution operators of non-autonomous evolution equations and obtain convergence analysis for our method. In Section 4, we present numerical results to demonstrate the accuracy and efficiency of our method. In addition, we investigate the dependence of KPP front speeds on the chaos (disorder) and flow intensities, especially in 3D time-dependent chaotic flows. Concluding remarks are made in Section 5. Finally, we collect several fundamental results for abstract linear evolution equations by semigroup theory in the Appendix.

2. Efficient Lagrangian methods in computing KPP front speeds

2.1. Computing principal eigenvalue via the Feynman-Kac formula

In this section, we develop Lagrangian interacting particle methods to compute KPP front propagation via the Feynman-Kac formula. We consider the linearized corrector equation of the KPP equation (1), where the velocity field $\mathbf{v}(t, \mathbf{x})$ is space-time periodic, mean zero, and divergence-free. To compute the KPP front speed $c^*(\mathbf{e})$ along direction \mathbf{e} , let w solve a linearized equation parameterized by $\lambda > 0$:

$$w_t = \mathcal{A}w := \kappa\Delta w + (2\lambda\mathbf{e} + \mathbf{v}) \cdot \nabla_{\mathbf{x}}w + (\kappa\lambda^2 + \lambda\mathbf{v} \cdot \mathbf{e} + \tau^{-1}f'(0))w, \quad (4)$$

with initial condition $w(\mathbf{x}, 0) = 1$. Then, the principal eigenvalue $\mu(\lambda)$ is given by

$$\mu(\lambda) = \lim_{t \rightarrow \infty} \frac{1}{t} \ln \int_{\mathbb{T}^d} w(t, \mathbf{x}) d\mathbf{x}. \quad (5)$$

The number $\mu(\lambda)$ is also the principal Lyapunov exponent of the parabolic equation (4), which is convex and superlinear in large λ [30, 47]. Finally, we compute the KPP front speed using the variational formula $c^*(\mathbf{e}) = \inf_{\lambda > 0} \mu(\lambda)/\lambda$.

To design Lagrangian particle methods, we decompose the operator \mathcal{A} in (4) into $\mathcal{A} = \mathcal{L} + \mathcal{C}$, where $\mathcal{L} := \kappa\Delta + (2\lambda\mathbf{e} + \mathbf{v}) \cdot \nabla_{\mathbf{x}}$ and $\mathcal{C} := c(t, \mathbf{x}) = (\kappa\lambda^2 + \lambda\mathbf{v} \cdot \mathbf{e} + \tau^{-1}f'(0))$. To approximate the operator \mathcal{L} , we define a SDE system as follows

$$d\mathbf{X}^{t,\mathbf{x}} = \mathbf{b}(t, \mathbf{X}^{t,\mathbf{x}})dt + \sqrt{2\kappa}d\mathbf{w}(t), \quad \mathbf{X}^{0,\mathbf{x}} = \mathbf{x}, \quad (6)$$

where the drift term $\mathbf{b} = 2\lambda\mathbf{e} + \mathbf{v}$ is determined by the advection field in the operator \mathcal{L} and $\mathbf{w}(t)$ is a d -dimensional Brownian motion. The principal eigenvalue $\mu(\lambda)$ of (4) can be represented via the Feynman-Kac formula as

$$\mu(\lambda) = \lim_{t \rightarrow \infty} \frac{1}{t} \ln \mathbb{E} \left(\exp \left(\int_0^t c(s, \mathbf{X}^{s,\mathbf{x}}) ds \right) \right), \quad (7)$$

where the expectation $\mathbb{E}[\cdot]$ is over randomness induced by the Brownian motion $\mathbf{w}(t)$.

If we apply the formula (5) to compute the principal eigenvalue $\mu(\lambda)$, we need to solve a parabolic-type PDE (4) using numerical methods, such as FEM and spectral method. When

the magnitude of velocity field is large and/or the dimension of spatial variables d is big (say $d = 3$), the FEM and spectral method become extremely expensive. The Feynman-Kac formula (7) provides an alternative strategy to design Lagrangian methods to compute the principal eigenvalue $\mu(\lambda)$, and thus allows us to compute the KPP front speeds. As we will demonstrate in Section 4, the proposed Lagrangian methods are efficient for computing KPP front speeds in 3D time-dependent chaotic flows.

Remark 2.1. When the velocity field in the KPP equation (1) is time-independent, construction of the Lagrangian method for computing KPP front speeds is straightforward. We simply replace the drift term \mathbf{b} in (6) and the potential c in (7) by their time-independent counterparts.

2.2. Feynman-Kac semigroups

Directly using the Feynman-Kac formula (7) and Monte Carlo method to compute the principal eigenvalue $\mu(\lambda)$ is unstable as the main contribution to $\mathbb{E}\left(\exp\left(\int_0^t c(s, \mathbf{X}^{s,\mathbf{x}})ds\right)\right)$ comes from sample paths that visit maximal or minimal points of the potential function c , which leads to inaccurate or even divergent results.

Accurate principal eigenvalue $\mu(\lambda)$ can be obtained by studying the convergence of the Feynman-Kac semigroup associated with the SDE system (6) and the potential c . Specifically, let $\mathcal{P}(\mathbb{T}^d)$ denote the set of probability measures over \mathbb{T}^d and $S = \mathcal{C}^\infty(\mathbb{T}^d)$. We define the evolution operator associated with the process $(\mathbf{X}^{t,\mathbf{x}})_{t \geq 0}$ in (6) as

$$(\nu)(P_t \phi) = \mathbb{E}_\nu[\phi(\mathbf{X}^{t,\mathbf{x}})], \quad \forall \nu \in \mathcal{P}(\mathbb{T}^d), \phi \in S. \quad (8)$$

Similarly, we define its weighted counterpart as

$$(\nu)(P_t^c \phi) = \mathbb{E}_\nu\left[\phi(\mathbf{X}^{t,\mathbf{x}}) \exp\left(\int_0^t c(s, \mathbf{X}^{s,\mathbf{x}})ds\right)\right], \quad \forall \nu \in \mathcal{P}(\mathbb{T}^d), \phi \in S. \quad (9)$$

In other words, infinitesimal generators of P_t and P_t^c are \mathcal{L} and $\mathcal{A} = \mathcal{L} + \mathcal{C}$, respectively.

Equipped with the definitions of the evolution operators P_t and P_t^c , we can define the Feynman-Kac semigroup Φ_t^c as follows

$$\Phi_t^c(\nu)(\phi) := \frac{(\nu)(P_t^c \phi)}{(\nu)(P_t^c 1)} = \frac{\mathbb{E}_\nu\left(\phi(\mathbf{X}^{t,\mathbf{x}}) \exp\left(\int_0^t c(s, \mathbf{X}^{s,\mathbf{x}})ds\right)\right)}{\mathbb{E}_\nu\left(\exp\left(\int_0^t c(s, \mathbf{X}^{s,\mathbf{x}})ds\right)\right)}. \quad (10)$$

One can easily verify that for all $\nu \in \mathcal{P}(\mathbb{T}^d)$ and $t_1, t_2 \in \mathbb{R}_+$, $\Phi_{t_1}^c(\Phi_{t_2}^c(\nu)) = \Phi_{t_1+t_2}^c(\nu)$. Thus, the family of maps $\{\Phi_t^c\}_{t \geq 0}$ is a measure-valued semigroup.

Notice that we use T to denote the period of the velocity in time. Therefore, we consider the Feynman-Kac semigroup for $t = nT, n \in \mathbb{N}$. Namely, we consider $\Phi_{nT}^c = (\Phi_T^c)^n$. One can easily verify the Feynman-Kac semigroup Φ_{nT}^c satisfies the following property, where the proof is a direct conclusion of Theorem 3.7 and Theorem 3.8.

Proposition 2.2. For any $\nu \in \mathcal{P}(\mathbb{T}^d)$ and $\phi \in S$, there exists $C > 0$ such that

$$\left| \Phi_{nT}^c(\nu)(\phi) - \int_\Omega \phi d\nu_c \right| \leq C \|\phi\| \exp(-\delta_c nT), \quad (11)$$

where $\delta_c = \inf\{\mu(\lambda) - \Re(z) : z \in \sigma(\mathcal{A}) \setminus \{\mu(\lambda)\}\} > 0$ is the spectral gap of the operator \mathcal{A} .

The exponential-decay property stated above ensures us to obtain an invariant measure ν_c for Φ_T^c from any initial measure ν . From the definition of ν_c , we know that $\Phi_T^c(\nu_c) = \nu_c$, which means that for any $\phi \in S$

$$\int_{\mathbb{T}^d} \phi d\nu_c = \left(\int_{\mathbb{T}^d} P_T^c 1 d\nu_c \right)^{-1} \int_{\mathbb{T}^d} P_T^c \phi d\nu_c. \quad (12)$$

Therefore, we can find that the principal eigenvalue of P_T^c is just $\int_{\mathbb{T}^d} P_T^c 1 d\nu_c$, which provides a feasible way to compute the principal eigenvalue.

2.3. Numerical discretization and resampling techniques

Let M be the number of time discretization interval for each period and $\Delta t = T/M$. We use the Euler-Maruyama scheme to discretize the SDE (6) and obtain

$$\mathbf{X}_{i+1} = \mathbf{X}_i + \mathbf{b}(t_i, \mathbf{X}_i)\Delta t + \sqrt{2\kappa\Delta t}\boldsymbol{\omega}_i, \quad (13)$$

where $t_i = i\Delta t$ and $\boldsymbol{\omega}_i$'s are i.i.d. d -dimensional standard Gaussian random variables. The numerical scheme (13) defines an evolution operator $P_i^{\Delta t}$ (also known as transition operator) as follows

$$P_i^{\Delta t}\phi(\mathbf{x}) = \mathbb{E}(\phi(\mathbf{X}_{i+1})|\mathbf{X}_i = \mathbf{x}). \quad (14)$$

The evolution operator $P_i^{\Delta t}$ describes how the values of a given function evolve in L_2 sense over one time step Δt . One can easily verify that

$$\|P_i^{\Delta t} - e^{\Delta t\mathcal{L}(t_i)}\|_{L_2} \leq C(\Delta t)^2, \quad (15)$$

where C is a positive constant [26]. Specially, when $\mathbf{b} = 0$, $P_i^{\Delta t} = e^{\Delta t\mathcal{L}(t_i)}$ for all i . Therefore, solving the SDE system (6) by the numerical scheme (13) provides a good approximation to the evolution operator $e^{\Delta t\mathcal{L}(t_i)}$, which plays an important role in the error estimate of our Lagrangian methods in Section 3.

In addition, we can define the approximation operator for P_t^c in (9). For instance, if we choose the left-point rectangular integration, we obtain

$$(\nu)(P_i^{\Delta t}e^{\Delta t\mathcal{C}(t_i)}\phi) = \mathbb{E}\left[\phi(\mathbf{X}_{i+1}) \exp(c(t_i, \mathbf{X}_{i+1})\Delta t) \mid \mathbf{X}_i \sim \nu\right], \quad i = 1, 2, \dots, M. \quad (16)$$

The time discretization for Feynman-Kac semigroup (10) reads:

$$\Phi_i^{c, \Delta t}(\nu)(\phi) = \frac{(\nu)(P_i^{\Delta t}e^{\Delta t\mathcal{C}(t_i)}\phi)}{(\nu)(P_i^{\Delta t}e^{\Delta t\mathcal{C}(t_i)}1)}, \quad i = 0, 1, 2, \dots, M-1. \quad (17)$$

It is difficult to obtain a closed-form solution to the evolution of probability measure in (17). Therefore, we approximate the evolution of probability measure in (17) by an N -interacting particle system (N -IPS) [28]. Let us introduce the notation $\mathcal{K}^{\Delta t} = \mathcal{K}^{\Delta t, M-1}\mathcal{K}^{\Delta t, M-2} \dots \mathcal{K}^{\Delta t, 0}$, where $\mathcal{K}^{\Delta t, i} = P_i^{\Delta t}e^{\Delta t\mathcal{C}(t_i)}$, $\Delta t = T/M$, and T is time period. We denote

$$\Phi^{\mathcal{K}^{\Delta t, i}}(\nu)(\phi) = \frac{(\nu)(\mathcal{K}^{\Delta t, i}\phi)}{(\nu)(\mathcal{K}^{\Delta t, i}1)} \quad (18)$$

the Feynman-Kac semigroup associated with the operator $\mathcal{K}^{\Delta t, i}$. Then, according to Lemma 3.6, it satisfies

$$\Phi^{\mathcal{K}^{\Delta t}} = \prod_{i=0}^{M-1} \Phi^{\mathcal{K}^{\Delta t, i}} = \Phi^{\mathcal{K}^{\Delta t, 0}} \Phi^{\mathcal{K}^{\Delta t, 1}} \dots \Phi^{\mathcal{K}^{\Delta t, M-1}}. \quad (19)$$

Suppose the Markov process $(\Theta, (\mathcal{F}_n)_{n \geq 0}, (\xi^n)_{n \geq 0}, \mathbb{P})$ is defined in the product space $(\mathbb{T}^d)^N$. For any initial probability measure $\pi_0 = \nu$, we approximate it by a N -particle system as

$$P(\xi^0 \in dz) = \prod_{p=1}^N \pi_0(dz^p). \quad (20)$$

Then, we evolve the N -particle system according to

$$P(\xi^n \in dz | \xi^{n-1} = \mathbf{x}) = \prod_{p=1}^N \Phi^{\mathcal{K}^{\Delta t}} \left(\frac{1}{N} \sum_{i=1}^N \delta_{x^i} \right) (dz^p) = \prod_{p=1}^N \left(\prod_{i=0}^{M-1} \Phi^{\mathcal{K}^{\Delta t, i}} \right) \left(\frac{1}{N} \sum_{i=1}^N \delta_{x^i} \right) (dz^p), \quad (21)$$

where $\mathbf{x} = (x^1, \dots, x^N)^T$ and n denotes the iteration number in the evolution of probability measure by the Feynman-Kac semigroup (17).

From Eq.(20), we can compute the evolution from ξ^{n-1} to ξ^n . It will be divided into M small steps. Let us denote $\xi_0^n = \xi^n$ for all n . Within each iteration stage $n-1$, we evolve the particles from $t=0$ to $t=T$ by the evolution operator $P_i^{\Delta t}$ and resample these particles according to weights determined by the potential function. Specifically, at $t_i = i\Delta t$, $i=0, \dots, M-1$, we evolve the particles ξ_i^{n-1} by the numerical scheme (13) and get $\tilde{\xi}_{i+1}^{n-1}$. Each particle is updated by

$$\tilde{\xi}_{i+1}^{p, n-1} = \xi_i^{p, n-1} + \mathbf{b}(t_i, \xi_i^{p, n-1})\Delta t + \sqrt{2\kappa\Delta t} \boldsymbol{\omega}_i^{p, n-1}, \quad p = 1, 2, \dots, N, \quad (22)$$

where $\boldsymbol{\omega}_i^{p, n-1}$ are i.i.d. d -dimensional standard Gaussian random variables.

Then, we resample the particles in $\tilde{\xi}_{i+1}^{n-1}$ according to the multinomial distribution with the weights

$$w_i^{p, n-1} = \frac{\exp(c(t_i, \tilde{\xi}_i^{p, n-1})\Delta t)}{\sum_{p=1}^N \exp(c(t_i, \tilde{\xi}_i^{p, n-1})\Delta t)}, \quad p = 1, \dots, N, \quad (23)$$

and obtain ξ_{i+1}^{n-1} .

The evolution of N -IPS from $(n-1)T$ to nT can be represented as follows

$$\begin{aligned} \xi_0^{n-1} &= (\xi_0^{1, n-1}, \dots, \xi_0^{N, n-1}) \longrightarrow \xi_1^{n-1} = (\xi_1^{1, n-1}, \dots, \xi_1^{N, n-1}) \longrightarrow \\ &\dots \longrightarrow \xi_M^{n-1} = (\xi_M^{1, n-1}, \dots, \xi_M^{N, n-1}) = \xi_0^n = (\xi_0^{1, n}, \dots, \xi_0^{N, n}). \end{aligned} \quad (24)$$

We know that the empirical distribution of the particles ξ_0^n will weakly converge to the distribution $\Phi_n^{\mathcal{K}^{\Delta t}}(\pi_0)$ as $N \rightarrow \infty$.

After obtaining the empirical distribution of the particles ξ_0^n , we can compute the principal eigenvalues. At the iteration stage n , we first define the change of the mass as follows

$$e_{i, n}^N = N^{-1} \sum_{p=1}^N \exp(c(t_i, \tilde{\xi}_i^{p, n-1})\Delta t). \quad (25)$$

Then, we compute the approximation of the principal eigenvalue by

$$\mu_{\Delta t}^n(\lambda) = (M\Delta t)^{-1} \sum_{i=1}^M \log \left(N^{-1} \sum_{p=1}^N \exp(c(t_i, \tilde{\xi}_i^{p,n-1})\Delta t) \right). \quad (26)$$

Finally, we give the complete algorithm in Algorithm 1. The performance of our method will be demonstrated in Section 4.

Algorithm 1 Algorithm for computing the principal eigenvalues of parabolic equations

Input: velocity field $\mathbf{v}(\mathbf{x}, t)$, potential $c(\mathbf{x}, t)$, number of N -IPS system (i.e., N), initial probability measure ν_0 , iteration number n , time period T , and time step $\Delta t = T/M$.

- 1: Generate N i.i.d. ν_0 -distributed random variables on $[0, 1]^d$: $\boldsymbol{\xi}_0^1 = (\xi_0^{1,1}, \dots, \xi_0^{N,1})$.
- 2: **for** $k = 1 : n$ **do**
- 3: **for** $i = 0 : M - 1$ **do**
- 4: Generate standard normal variables ω_i^k and compute $\tilde{\boldsymbol{\xi}}_{i+1}^{k-1}$ according to $\boldsymbol{\xi}_i^{k-1}$ by (22).
- 5: Compute the pointwise value $\mathbf{S} = (e^{C^1}, \dots, e^{C^N})$, where $C^i = c(i\Delta t, \tilde{\boldsymbol{\xi}}_i^{k-1})\Delta t$.
- 6: Compute weights $\mathbf{w} = (w^1, \dots, w^N) = \mathbf{S}/\text{SUM}(\mathbf{S})$ and $\mathbf{E}_{k,i} = \frac{1}{\Delta t} \log(\text{mean}(\mathbf{S}))$.
- 7: Resample $\tilde{\boldsymbol{\xi}}_{i+1}^{k-1}$ according to multinomial distribution with weight \mathbf{w} , and get $\boldsymbol{\xi}_{i+1}^{k-1}$.
- 8: **end for**
- 9: Compute $\mathbf{E}_k = M^{-1} \sum_{i=0}^{M-1} (\mathbf{E}_{k,i})$ and define $\boldsymbol{\xi}_M^{k-1} = \boldsymbol{\xi}_0^k$.
- 10: **end for**

Output: The approximate invariant distribution $\Phi_n^{\mathcal{K}^{\Delta t}}(\nu)$ -distributed variable $\boldsymbol{\xi}_n^0$ and approximate eigenvalue $\tilde{\lambda}_{n,\Delta t} = n^{-1} \sum_{k=1}^n \mathbf{E}_k$;

Remark 2.1. When the flow is time-independent, we can view it as a periodic flow with any given period T . The principal eigenvalue calculated by (5) will be the same with any $T > 0$. Hence the numerical schemes and the convergence analysis proposed in time-dependent flow can be applied by assigning $T = \Delta t$ and $M = 1$.

3. Convergence analysis of the Lagrangian particle method

In this section, we will prove the convergence of the Lagrangian particle method in computing KPP front speed. We divide the analysis into two parts. The first part studies the approximation of the evolution of parabolic operators by using an operator splitting method. The second part studies the error estimate of the Lagrangian particle method in computing the principal eigenvalue of parabolic operators.

3.1. Approximation of the evolution of parabolic operators

We first rewrite the linearized corrector equation of the KPP equation (4) into the following non-autonomous parabolic equation

$$w_t = \kappa \Delta_{\mathbf{x}} w + \mathbf{b}(t, \mathbf{x}) \cdot \nabla_{\mathbf{x}} w + c(t, \mathbf{x}) w, \quad \mathbf{x} = (x_1, \dots, x_d)^T \in \mathbb{T}^d = [0, 1]^d, \quad t \in [0, T], \quad (27)$$

where the initial condition $w(0, \mathbf{x}) = w_0$, $\mathbf{b}(t, \mathbf{x}) = 2\lambda\mathbf{e} + \mathbf{v}$, $c(t, \mathbf{x}) = \kappa\lambda^2 + \lambda\mathbf{v} \cdot \mathbf{e} + \tau^{-1}f'(0)$, and T is final computational time. Since the velocity $\mathbf{v} = \mathbf{v}(t, \mathbf{x})$ is space-time periodic, so do $\mathbf{b}(t, \mathbf{x})$ and $c(t, \mathbf{x})$. We assume the period of $\mathbf{b}(t, \mathbf{x})$ and $c(t, \mathbf{x})$ is one in each dimension and they are smooth functions. For notational simplicity, we define

$$\mathcal{A}(t) = \mathcal{L}(t) + \mathcal{C}(t), \quad (28)$$

where $\mathcal{L}(t) := \kappa\Delta_{\mathbf{x}} + \mathbf{b}(t, \mathbf{x}) \cdot \nabla_{\mathbf{x}}$ and $\mathcal{C}(t) = c(t, \mathbf{x})$. The operator $\mathcal{A}(t)$ has a real isolated principal eigenvalue $\mu(\lambda)$ [17]. We aim to obtain error estimates of our Lagrangian method in approximating the principal eigenvalue $\mu(\lambda)$. To this end, we study the approximation the solution operator for the parabolic equation (27) by using an operator splitting method.

We define the solution operator $\mathcal{U}(t, s)$ corresponding to the parabolic equation (27), which satisfies the following properties:

1. $\mathcal{U}(s, s) = Id$, for any $s \geq 0$;
2. $\mathcal{U}(t, r) \circ \mathcal{U}(r, s) = \mathcal{U}(t, s)$, for any $t \geq r \geq s \geq 0$;
3. $\frac{d}{dt}\mathcal{U}(t, s)w_0 = \mathcal{A}(t)\mathcal{U}(t, s)w_0$, for any $t \geq s \geq 0, w_0 \in L^2([0, 1]^d)$.

The solution operator $\mathcal{U}(t, s)$ enables us to study the evolution of parabolic operator in (27), e.g., the principal eigenvalue of $\mathcal{U}(T, 0)$ gives the principal eigenvalue of the parabolic operator $\mathcal{A}(t)$. It has been proven that the principal eigenvalue of $\mathcal{U}(T, 0)$ exists and is real [17]. It is difficult to obtain a closed-form for the solution operator $\mathcal{U}(T, 0)$. Therefore, we approximate the solution operator $\mathcal{U}(T, 0)$ by using an operator splitting method.

We set $t_i = i\Delta t$ with $\Delta t = \frac{T}{M}$ and consider the following parabolic equation with freezing time coefficients.

$$w_t = \kappa\Delta_{\mathbf{x}}w + \mathbf{b}(t_i, \mathbf{x}) \cdot \nabla_{\mathbf{x}}w + c(t_i, \mathbf{x})w, \quad t_i < t \leq t_{i+1}, \quad i \geq 0. \quad (29)$$

The corresponding solution operator can be formally represented as

$$w(t) = e^{(t-t_i)(\mathcal{L}+\mathcal{C})(t_i)} \prod_{k=0}^{i-1} e^{\Delta t(\mathcal{L}+\mathcal{C})(t_k)} w_0, \quad t_i \leq t < t_{i+1}. \quad (30)$$

Furthermore, we can apply the first-order Lie-Trotter operator splitting method to approximate the solution operator defined in (30) and obtain

$$w(t) = e^{(t-t_i)\mathcal{L}(t_i)} e^{(t-t_i)\mathcal{C}(t_i)} \prod_{k=0}^{i-1} e^{\Delta t\mathcal{L}(t_j)} e^{\Delta t\mathcal{C}(t_j)} w_0, \quad t_i \leq t < t_{i+1}. \quad (31)$$

We will prove the solution operator $\prod_{j=0}^{M-1} e^{\Delta t\mathcal{L}(t_j)} e^{\Delta t\mathcal{C}(t_j)}$ obtained by the Lie-Trotter operator splitting method converges to the solution operator $\mathcal{U}(T, 0)$ in certain operator norm as Δt approaches zero. As a consequence of this convergence result, we can further prove the convergence of the principal eigenvalue associated with these two solution operators.

To make our paper self-contained, we collect several fundamental results for abstract linear evolution equations by semigroup theory in Appendix A. We begin with following lemma, which is as a special case of Theorem 1 in [41].

Lemma 3.1. Let t be fixed. If $\mathbf{b}(t, \mathbf{x})$ and $c(t, \mathbf{x})$ are smooth and bounded, then the operator $\mathcal{A}(t)$ defined in (28) is a strongly elliptic operator on \mathbb{T}^d . Moreover, $\mathcal{A}(t)$ generates an analytic semigroup $e^{\mathcal{A}(t)}$ in $L^p(\mathcal{D})$, for all $1 \leq p \leq \infty$.

We will prove that, in our non-autonomous parabolic equation setting, the assumptions made in Appendix A are all satisfied, so we can obtain the error of the operator splitting method in approximation the non-autonomous parabolic operator.

We first prove that the operator \mathcal{A} defined in (28) satisfies a Hölder continuous condition.

Lemma 3.2. Suppose $\mathbf{b}(t, \mathbf{x})$ and $c(t, \mathbf{x})$ in the operator $\mathcal{A}(t)$ are bounded, smooth and periodic in each component of \mathbf{x} , and uniformly Hölder continuous in t , i.e., for any $t, s \in \mathbb{R}^+$,

$$\|\mathbf{b}(t, \mathbf{x}) - \mathbf{b}(s, \mathbf{x})\| \leq C_1|t - s|^\beta, \quad |c(t, \mathbf{x}) - c(s, \mathbf{x})| \leq C_1|t - s|^\beta, \quad (32)$$

for some positive C_1 and β . Let $v \in \mathcal{D}(\mathcal{A}(\cdot)) = H^2(\mathbb{T}^d)$ is periodic. Then, for any $0 < s \leq \tau$, there exists $\gamma_1 > 0$, such that

$$\|\mathcal{A}(\tau)v - \mathcal{A}(s)v\|_{L^2} \leq C_2(\tau - s)^\beta \|(\mathcal{A}(t) - \gamma_1)v\|_{L^2}^{1/2} \|v\|_{L^2}^{1/2}, \quad (33)$$

for any $t \in \mathbb{R}^+$. Specifically, if $\mathbf{b}(t, \mathbf{x}) = 0$, then

$$\|\mathcal{A}(\tau)v - \mathcal{A}(s)v\|_{L^2} \leq C_3(\tau - s)^\beta \|v\|_{L^2}. \quad (34)$$

Proof. We first consider the case when $\mathbf{b}(t, \mathbf{x}) \neq 0$. By using the uniformly Hölder continuous conditions for $b(t, \mathbf{x})$ and $c(t, \mathbf{x})$, we have

$$\begin{aligned} \|\mathcal{A}(\tau)v - \mathcal{A}(s)v\|_{L^2} &= \|(\mathbf{b}(\tau, \mathbf{x}) - \mathbf{b}(s, \mathbf{x})) \cdot \nabla_{\mathbf{x}}v + (c(\tau, \mathbf{x}) - c(s, \mathbf{x}))v\|_{L^2} \\ &\leq C_1(t - s)^\beta (\|\nabla_{\mathbf{x}}v\|_{L^2} + \|v\|_{L^2}). \end{aligned} \quad (35)$$

For the operator $\mathcal{A}(t)$, we claim that there exists $\gamma_1 > 0$ such that,

$$\|(\mathcal{A}(t) - \gamma_1)v\|_{L^2} > C(\kappa, \mathbf{b}, c) (\|\Delta_{\mathbf{x}}v\|_{L^2} + \|v\|_{L^2}), \quad \forall v \in \mathcal{D}(\mathcal{A}(\cdot)), \quad (36)$$

where the constant $C(\kappa, \mathbf{b}, c)$ depends on κ , $\mathbf{b}(t, \mathbf{x})$ and $c(t, \mathbf{x})$.

We prove the statement in (36) before move to the main results. Let $c_{\gamma_1} = c - \gamma_1$ and assume $\|\mathbf{b}(t, \mathbf{x})\| \leq M_1$, $|c(t, \mathbf{x})| \leq M_2$, $\|\nabla_{\mathbf{x}}c(t, \mathbf{x})\| \leq M_3$. We know that

$$\begin{aligned} \|(\mathcal{A}(t) - \gamma_1)v\|_{L^2} &= \|(\kappa\Delta_{\mathbf{x}} + \mathbf{b}(t, \mathbf{x}) \cdot \nabla_{\mathbf{x}} + c_{\gamma_1}(t, \mathbf{x}))v\|_{L^2} \\ &\geq \|(\kappa\Delta_{\mathbf{x}} + c_{\gamma_1}(t, \mathbf{x}))v\|_{L^2} - \|\mathbf{b}(t, \mathbf{x}) \cdot \nabla_{\mathbf{x}}v\|_{L^2}. \end{aligned} \quad (37)$$

For the term $\|(\kappa\Delta_{\mathbf{x}} + c_{\gamma_1}(t, \mathbf{x}))v\|_{L^2}$, the periodic condition of v implies that

$$\begin{aligned} &\|(\kappa\Delta_{\mathbf{x}} + c_{\gamma_1}(t, \mathbf{x}))v\|_{L^2}^2 \\ &= \|\kappa\Delta_{\mathbf{x}}v\|_{L^2}^2 + \|c_{\gamma_1}(t, \mathbf{x})v\|_{L^2}^2 - 2\langle \kappa\nabla_{\mathbf{x}}v, c_{\gamma_1}(t, \mathbf{x})\nabla_{\mathbf{x}}v \rangle_{L^2} - 2\langle \kappa\nabla_{\mathbf{x}}v, v\nabla_{\mathbf{x}}c(t, \mathbf{x}) \rangle_{L^2} \end{aligned} \quad (38)$$

Notice that if we choose $\gamma_1 = \frac{2M_1^2}{\kappa} + M_2$, then we obtain

$$-2\langle \kappa\nabla_{\mathbf{x}}v, c_{\gamma_1}(t, \mathbf{x})\nabla_{\mathbf{x}}v \rangle_{L^2} \geq 4\kappa(\gamma_1 - M_2)\|\nabla_{\mathbf{x}}v\|_{L^2}^2 \geq 4\|\mathbf{b}(t, \mathbf{x}) \cdot \nabla_{\mathbf{x}}v\|_{L^2}. \quad (39)$$

In addition, we have

$$2\langle \kappa \nabla_{\mathbf{x}} v, v \nabla_{\mathbf{x}} c(t, \mathbf{x}) \rangle_{L^2} \leq 2\kappa M_3 \|\nabla_{\mathbf{x}} v\|_{L^2} \|v\|_{L^2} \leq 2\kappa M_3 C \|\Delta_{\mathbf{x}} v\|_{L^2}^{\frac{1}{2}} \|v\|_{L^2}^{\frac{3}{2}}. \quad (40)$$

Here, we use the fact that $\|\nabla_{\mathbf{x}} v\|_{L^2} \leq C \|\Delta_{\mathbf{x}} v\|_{L^2}^{\frac{1}{2}} \|v\|_{L^2}^{\frac{1}{2}}$, which is the moment inequality in interpolation theory; see Theorem 5.34 of [11]. If we take γ_1 large enough such that $4\left(\frac{\gamma_1 - M_2}{3}\right)^{\frac{3}{4}} \kappa^{\frac{1}{4}} \geq 2\kappa M_3 C$, we get that

$$\|\kappa \Delta_{\mathbf{x}} v\|_{L^2}^2 + \|c_{\gamma_1}(t, \mathbf{x}) v\|_{L^2}^2 \geq 2\kappa M_3 C \|\Delta_{\mathbf{x}} v\|_{L^2}^{\frac{1}{2}} \|v\|_{L^2}^{\frac{3}{2}} \geq 2\langle \kappa \nabla_{\mathbf{x}} v, v \nabla_{\mathbf{x}} c(t, \mathbf{x}) \rangle_{L^2}. \quad (41)$$

Substituting the estimates (39)-(41) into (38), we obtain

$$\|(\kappa \Delta_{\mathbf{x}} + c_{\gamma_1}(t, \mathbf{x})) v\|_{L^2} \geq 2\|\mathbf{b}(t, \mathbf{x}) \cdot \nabla_{\mathbf{x}} v\|_{L^2}. \quad (42)$$

Thus, from (37) we get that

$$\|(\mathcal{A}(t) - \gamma_1) v\|_{L^2} \geq \frac{1}{2} \|(\kappa \Delta_{\mathbf{x}} + c_{\gamma_1}(t, \mathbf{x})) v\|_{L^2}. \quad (43)$$

Using the same argument, we can prove that for γ_1 large enough,

$$\|(\kappa \Delta_{\mathbf{x}} + c_{\gamma_1}(t, \mathbf{x})) v\|_{L^2} \geq \hat{C} (\|\Delta_{\mathbf{x}} v\|_{L^2} + \|v\|_{L^2}). \quad (44)$$

Finally, using the moment inequality we prove the statement in (33).

The case when $\mathbf{b}(t, \mathbf{x}) = 0$ is simple since we have

$$\|\mathcal{A}(\tau) v - \mathcal{A}(s) v\|_{L^2} = \|(c(\tau, \mathbf{x}) - c(s, \mathbf{x})) v\|_{L^2} \leq C_3 (t - s)^{\beta} \|v\|_{L^2}. \quad (45)$$

□

We then verify the operators $\mathcal{L}(t)$ and $\mathcal{C}(t)$ defined in (28) satisfy the assumption Appendix A.11. Given $\tau \geq 0$, we assume the bounded conditions as follows

$$\|e^{\tau \mathcal{L}(t)}\|_{L^2} \leq 1, \quad \|e^{\tau \mathcal{C}(t)}\|_{L^2} \leq 1, \quad \|e^{\tau(\mathcal{L}(t) + \mathcal{C}(t))}\|_{L^2} \leq 1. \quad (46)$$

Lemma 3.3. Suppose $\mathbf{b}(t, \mathbf{x})$ and $c(t, \mathbf{x})$ in the operator \mathcal{A} satisfy the same assumption as that in Lemma 3.2. Then, there exists $\gamma_2 > 0$ such that, for any periodic $v \in L^2(\mathbb{T}^d)$, commutator of \mathcal{L} and \mathcal{C} acting on v follows,

$$\|[\mathcal{L}(t), \mathcal{C}(t)] v\|_{L^2} \leq C_1 \|(\mathcal{L}(t) - \gamma_2) v\|_{L^2}^{\frac{1}{2}} \|v\|_{L^2}^{\frac{1}{2}}, \quad \forall t \geq 0. \quad (47)$$

Proof. We first observe that, for any v periodic in $L^2(\mathbb{T}^d)$,

$$\begin{aligned} \|[\mathcal{L}(t), \mathcal{C}(t)] v\|_{L^2} &= \|\mathcal{L}(t)(\mathcal{C}(t)v) - \mathcal{C}(t)(\mathcal{L}(t)v)\|_{L^2}, \\ &= \|(\kappa \Delta_{\mathbf{x}} c(t, \mathbf{x}) + \mathbf{b}(t, \mathbf{x}) \cdot \nabla_{\mathbf{x}} c(t, \mathbf{x})) v + 2\kappa \nabla_{\mathbf{x}} c(t, \mathbf{x}) \cdot \nabla v\|_{L^2}, \\ &\leq (\kappa M_4 + M_1 M_3) \|v\|_{L^2} + 2\kappa M_3 \|\nabla_{\mathbf{x}} v\|_{L^2}, \end{aligned} \quad (48)$$

where $\|\mathbf{b}(t, \mathbf{x})\| \leq M_1$, $\|\nabla_{\mathbf{x}} c(t, \mathbf{x})\| \leq M_3$, and $|\Delta_{\mathbf{x}} c(t, \mathbf{x})| \leq M_4$.

Following the same procedure as in the proof of Lemma 3.2, we have

$$\|(\mathcal{L}(t) - \gamma_1) v\|_{L^2} \geq C(\kappa, \mathbf{b}) (\|\Delta_{\mathbf{x}} v\|_{L^2} + \|v\|_{L^2}). \quad (49)$$

Using the fact that $\|\nabla_{\mathbf{x}} v\|_{L^2} \leq C \|\Delta_{\mathbf{x}} v\|_{L^2}^{\frac{1}{2}} \|v\|_{L^2}^{\frac{1}{2}}$, we finally prove the assertion in (47). □

Remark 3.1. If the bounded conditions (46) for $\mathcal{L}(t)$ and $\mathcal{C}(t)$ do not hold, we can shift the operators by a constant so that the shifted operators satisfy the bounded condition. Shift the operator by a constant will not affect the commutator in (47).

Now we are in the position to present the main result in approximating the solution operator $\mathcal{U}(t, s)$ for the parabolic equation (27).

Theorem 3.4. The solution operator (30) has the following error in approximating the solution operator $\mathcal{U}(T, 0)$ in L^2 operator norm

$$\|\mathcal{U}(T, 0) - \prod_{k=0}^{M-1} e^{\Delta t \mathcal{A}(k\Delta t)}\|_{L^2(\mathbb{T}^d)} \leq C_1(T)(\Delta t)^{\beta-\frac{1}{2}}, \quad (50)$$

where $T > 0$, M is an integer, and $\Delta t = \frac{T}{M}$. In addition, the Lie-Trotter operator splitting method has the following error in approximating the solution operator (30)

$$\left\| \prod_{k=0}^{M-1} e^{\Delta t \mathcal{A}(k\Delta t)} - \prod_{k=0}^{M-1} e^{\Delta t \mathcal{L}(k\Delta t)} e^{\Delta t \mathcal{C}(k\Delta t)} \right\|_{L^2(\mathbb{T}^d)} \leq C_2(T)(\Delta t)^{\frac{1}{2}}. \quad (51)$$

Proof. We take $\gamma = \max(\gamma_1, \gamma_2)$, where γ_1 and γ_2 are defined in Lemma 3.2 and Lemma 3.3 respectively. Let $\mathcal{U}_\gamma(t, s) = e^{-\gamma(t-s)}\mathcal{U}(t, s)$ be the solution operator that corresponds to the parabolic equation (27) with $\mathcal{A}_\gamma(t) = \mathcal{A}(t) - \gamma$ and $\mathcal{L}_\gamma(t) = \mathcal{L}(t) - \gamma$. Then, we have

$$\mathcal{U}(T, 0) - \prod_{k=0}^{M-1} e^{\Delta t \mathcal{A}(k\Delta t)} = e^{\gamma T} (U_\gamma(T, 0) - \prod_{k=0}^{M-1} e^{\Delta t \mathcal{A}_\gamma(k\Delta t)}) \quad (52)$$

The statement in (50) is proved according to Theorem Appendix A.9.

For the Lie-Trotter operator splitting method, we know that

$$\prod_{k=0}^{M-1} e^{\Delta t \mathcal{A}(k\Delta t)} - \prod_{k=0}^{M-1} e^{\Delta t \mathcal{L}(k\Delta t)} e^{\Delta t \mathcal{C}(k\Delta t)} = e^{\gamma T} \left(\prod_{k=0}^{M-1} e^{\Delta t \mathcal{A}_\gamma(k\Delta t)} - \prod_{k=0}^{M-1} e^{\Delta t \mathcal{L}_\gamma(k\Delta t)} e^{\Delta t \mathcal{C}(k\Delta t)} \right) \quad (53)$$

Now according to the Lemma 3.2 and 3.3, $\mathcal{A}_\gamma(k\Delta t) = \mathcal{L}_\gamma(k\Delta t) + \mathcal{C}(k\Delta t)$ and \mathcal{L}_γ and \mathcal{C} satisfy the assumptions Appendix A.10 and Appendix A.11. Thus, applying Theorem Appendix A.12 and Theorem Appendix A.13, we can prove the estimate (51). \square

The convergence of $\mathcal{K}^{\Delta t}$ in the operator norm $\mathcal{L}(L^2, H^1)$ has been proved in [2]. In Theorem 3.4 we obtain the convergence of $\mathcal{K}^{\Delta t}$ in the operator norm $\mathcal{L}(L^2)$. Finally, we can obtain the error estimate for the principal eigenvalue.

Theorem 3.5. Let $e^{\mu(\lambda)T}$ and $e^{\mu_{\Delta t}(\lambda)T}$ denote the principal eigenvalue of the solution operator $\mathcal{U}(T, 0)$ and the approximated solution operator $\prod_{k=0}^{M-1} e^{\Delta t \mathcal{L}(k\Delta t)} e^{\Delta t \mathcal{C}(k\Delta t)}$, respectively. Then, we have the error estimate as follows:

$$|e^{\mu(\lambda)T} - e^{\mu_{\Delta t}(\lambda)T}| \leq C_1(T)(\Delta t)^{\beta-\frac{1}{2}} + C_2(T)(\Delta t)^{\frac{1}{2}}. \quad (54)$$

Hence, $|\mu(\lambda) - \mu_{\Delta t}(\lambda)| = O((\Delta t)^{\min(\beta-\frac{1}{2}, \frac{1}{2})})$.

Proof. According to the standard spectral theorem [21], the principal eigenvalue $e^{\mu(\lambda)}$ for the solution operator $\mathcal{U}(T, 0)$ and the principal eigenvalue $e^{\mu_{\Delta t}(\lambda)}$ for the approximated solution operator $\prod_{k=0}^{M-1} e^{\Delta t \mathcal{L}(k\Delta t)} e^{\Delta t \mathcal{C}(k\Delta t)}$ satisfy

$$|e^{\mu(\lambda)T} - e^{\mu_{\Delta t}(\lambda)T}| \leq C_3 \left\| U(T, 0) - \prod_{k=0}^{N-1} e^{\Delta t \mathcal{L}(k\Delta t)} e^{\Delta t \mathcal{C}(k\Delta t)} \right\|_{L^2(\mathbb{T}^d)}. \quad (55)$$

By using triangle inequality for the right hand side of (55) and the estimated results from Theorem 3.4, we can get the error estimate (54). \square

If $b(t, \mathbf{x})$ and $c(t, \mathbf{x})$ in the operator \mathcal{A} are uniformly Lipschitz, then the error of the principal eigenvalue obtained by the Lie-Trotter operator splitting method is $O((\Delta t)^{\frac{1}{2}})$.

3.2. Analysis of the Lagrangian particle method

We consider the Feynman-Kac semigroup $\Phi^{\mathcal{A}}$ associated with an arbitrary operator \mathcal{A} . The action of the Feynman-Kac semigroup $\Phi^{\mathcal{A}}$ on a probability measure ν is defined by

$$\Phi^{\mathcal{A}}(\nu)(\phi) = \frac{(\nu)(\mathcal{A}\phi)}{(\nu)(\mathcal{A}1)}, \quad \forall \phi \in L^2(\mathbb{T}^d). \quad (56)$$

Moreover, we denote $\Phi_n^{\mathcal{A}} = (\Phi^{\mathcal{A}})^n$. The Feynman-Kac semigroup operation satisfies the following property.

Lemma 3.6. For any operators \mathcal{A}, \mathcal{B} in $\mathcal{L}(L^2(\mathbb{T}^d))$, $\Phi^{\mathcal{A}\mathcal{B}} = \Phi^{\mathcal{B}}\Phi^{\mathcal{A}}$.

Proof. Let ν be a probability measure and ϕ be a function in $L^2(\mathbb{T}^d)$. Then, we can easily verify that

$$\begin{aligned} \Phi^{\mathcal{A}\mathcal{B}}(\nu)(\phi) &= \frac{(\nu)(\mathcal{A}\mathcal{B}\phi)}{(\nu)(\mathcal{A}\mathcal{B}1)} = \frac{(\nu)(\mathcal{A}\mathcal{B}\phi)}{(\nu)(\mathcal{A}1)} \frac{(\nu)(\mathcal{A}1)}{(\nu)(\mathcal{A}\mathcal{B}1)}, \\ &= \frac{\Phi^{\mathcal{A}}(\nu)(\mathcal{B}\phi)}{\Phi^{\mathcal{A}}(\nu)(\mathcal{B}1)} = \Phi^{\mathcal{B}}\Phi^{\mathcal{A}}(\nu)(\phi). \end{aligned} \quad (57)$$

\square

Recall the operator $\Phi_n^{\mathcal{K}^{\Delta t}}$ defined in (19) is a composition of the Feynman-Kac semigroup $\Phi^{\mathcal{K}^{\Delta t, i}}$ associated with the operator $\mathcal{K}^{\Delta t, i}$; see (18). In the sequel, we will prove the operator $\Phi_n^{\mathcal{K}^{\Delta t}}$ satisfies the uniform minorization and boundedness condition with respect to Δt , which guarantees the existence of an invariant measure.

Theorem 3.7. There exists a probability measure η so that the operator $\mathcal{K}^{\Delta t}$ satisfies a uniform minorization and boundedness condition as follows

$$\epsilon\eta(\phi) \leq \mathcal{K}^{\Delta t}(\phi)(\mathbf{x}) \leq \gamma\eta(\phi), \quad \forall \mathbf{x} \in \mathbb{T}^d, \forall \phi \in L^2(\mathbb{T}^d), \quad (58)$$

where $0 < \epsilon < \gamma$ is independent with Δt . Moreover, when $\Delta t \rightarrow 0$ the limit operator is just the exact solution operator $\mathcal{U}(T, 0)$, which also satisfies this uniform minorization and boundedness condition.

Proof. We first define an operator $P^{\Delta t} = \prod_{i=0}^{M-1} P_{t_i}^{\Delta t}$, which corresponds to the case when $c(t, \mathbf{x}) = 0$ in Eq.(27). Since $c(t, \mathbf{x})$ is bounded (i.e. $c_1 \leq c(t, \mathbf{x}) \leq c_2$), one can easily obtain the following estimate based on the Feynman-Kac formula

$$P^{\Delta t}(\phi)e^{c_1 T} \leq \mathcal{K}^{\Delta t}(\phi) \leq P^{\Delta t}(\phi)e^{c_2 T}. \quad (59)$$

Thus, to estimate the bounds for $\mathcal{K}^{\Delta t}$, we only need to study the operator $P^{\Delta t}$. Moreover, it is sufficient to prove that there exist a probability measure η and a constant $\epsilon > 0$ so that for any indicator function of a Borel set $S \subset \mathbb{T}^d$ the following result holds

$$\mathbb{P}(\mathbf{X}_M \in S | \mathbf{X}_0 = \mathbf{x}) \geq \epsilon \eta(S), \quad (60)$$

where \mathbf{X}_i are defined in Eq.(13) as the numerical solution to the SDE (6). The idea of the proof is to explicitly rewrite \mathbf{X}_M as a perturbation of the reference evolution corresponding to $\mathbf{b} = 0$. According to the SDE scheme (13), we have

$$\mathbf{X}_M = \mathbf{X}_0 + \mathbf{G}_M + \mathbf{F}_M, \quad (61)$$

where

$$\mathbf{G}_M = \sqrt{2\kappa\Delta t} \sum_{i=0}^{M-1} \boldsymbol{\omega}_i, \quad \text{and,} \quad \mathbf{F}_M = \Delta t \sum_{i=0}^{M-1} \mathbf{b}(i\Delta t, \mathbf{X}_i). \quad (62)$$

We know that $|\mathbf{F}_m| \leq T \|\mathbf{b}\|_{L^\infty}$ and \mathbf{G}_M is a Gaussian random variable with covariance matrix $2\kappa T \text{Id}_d$. Therefore

$$\begin{aligned} \mathbb{P}(\mathbf{X}_M \in S | \mathbf{X}_0 = \mathbf{x}) &\geq \mathbb{P}(\mathbf{G}_M \in S - \mathbf{x} - \mathbf{F}_M) \\ &= \left(\frac{1}{2\pi\kappa T}\right)^{d/2} \int_{S - \mathbf{x} - \mathbf{F}_m} \exp\left(-\frac{|\mathbf{y}|^2}{2\kappa T}\right) d\mathbf{y}. \end{aligned} \quad (63)$$

Since the state space \mathbb{T}^d is compact, we can find $R > 0$ such that $|\mathbf{x} + \mathbf{F}_M| \leq R$ for all $\mathbf{x} \in \mathbb{T}^d$. Thus, we define the probability measure η as

$$\eta(S) = Z_R^{-1} \inf_{|Q| \leq R} \int_{S+Q} \exp\left(-\frac{|\mathbf{y}|^2}{2\kappa T}\right) d\mathbf{y}, \quad \forall S \subset \mathbb{T}^d, \quad (64)$$

where Z_R is a normalization constant. Setting $\epsilon = Z_R(4\pi\kappa T)^{-d/2}$, we can easily verify that $\eta(S) \geq Z_R^{-1} \exp(-\frac{|R+1|^2}{2\kappa T})|S|$, which satisfies a uniform minorization condition.

The uniform boundedness condition is automatically satisfied since η has a positive density with respect to Lebesgue measure.

The situation when the exact solution operator is considered can be samely proved by changing Eq.(61) into an Ito integration form

$$\mathbf{X}^{T, \mathbf{x}} = \mathbf{X}^{0, \mathbf{x}} + \int_0^T \mathbf{b}(t, \mathbf{X}^{t, \mathbf{x}}) dt + \int_0^T \sqrt{2\kappa} d\mathbf{w}(t) \quad (65)$$

and then go through the same procedure. \square

We now represent an important result that ensures the existence of the limiting measure for the discretized Feymann-Kac dynamics. The detailed proof of Theorem 3.8 can be found in [25] or Corollary 2.5 in [27].

Theorem 3.8. Suppose the minorization and boundedness conditions (58) hold true. Then, the $\Phi_n^{\mathcal{K}^{\Delta t}}$ admits an invariant measure $\nu_{\Delta t}$, whose density function is the eigenfunction of the operator $(\mathcal{K}^{\Delta t})^*$, adjoint operator of the solution operator $\mathcal{K}^{\Delta t}$. Moreover, for any initial distribution $\nu_0 \in \mathcal{P}(\mathbb{T}^d)$

$$\|\Phi_n^{\mathcal{K}^{\Delta t}}(\nu_0) - \nu_{\Delta t}\|_{TV} \leq 2(1 - \frac{\epsilon}{\gamma})^n, \quad (66)$$

where $\|\cdot\|_{TV}$ is the total variation norm and $0 < \epsilon < \gamma$ are from the minorization and boundedness conditions introduced in (58). This is also true when changing $\mathcal{K}^{\Delta t}$ to the exact solution operator $\mathcal{U}(T, 0)$.

Corollary 3.9. The principal eigenvalue $\mu_{\Delta t}$ of $\mathcal{K}^{\Delta t}$ satisfies the following relation

$$e^{\mu_{\Delta t}(\lambda)T} = \nu_{\Delta t} \mathcal{K}^{\Delta t} 1 = \Phi_n^{\mathcal{K}^{\Delta t}}(\nu_0) \mathcal{K}^{\Delta t} 1 + \rho_n, \quad (67)$$

where ν_0 is any bounded non-negative initial probability measure, T is the period of the time parameter, and $\rho_n = O(1 - \frac{\epsilon}{\gamma})^n$.

Proof. Lemma 3.8 implies that for any bounded non-negative measure ν_0 , the measure $\Phi_n^{\mathcal{K}^{\Delta t}}(\nu_0)$ converges to an invariant measure $\nu_{\Delta t}$ in the weak sense, that is

$$\nu_{\Delta t} \phi := \int_{\mathbb{T}^d} \phi d\nu_{\Delta t} = \Phi_n^{\mathcal{K}^{\Delta t}}(\nu_0)(\phi) + O(1 - \frac{\epsilon}{\gamma})^n, \quad (68)$$

for any bounded non-negative measurable function ϕ .

Then, we take $\phi = \mathcal{K}^{\Delta t} 1$. From the fact that the density function of $\nu_{\Delta t}$ is the eigenfunction of the operator $(\mathcal{K}^{\Delta t})^*$, we get that

$$\nu_{\Delta t}(\mathcal{K}^{\Delta t} 1) = ((\mathcal{K}^{\Delta t})^* \nu_{\Delta t}) 1 = e^{\mu_{\Delta t}(\lambda)T} (\nu_{\Delta t} 1) = e^{\mu_{\Delta t}(\lambda)T}. \quad (69)$$

Thus we finish the proof. \square

Now we compute the principal eigenvalue $\mu_{\Delta t}(\lambda)$.

Lemma 3.10. Denote $\nu_{\Delta t}^k = \prod_{i=0}^{k-1} \Phi^{\mathcal{K}^{\Delta t, i}} \nu_{\Delta t}$. Let $e_k = (\nu_{\Delta t}^k)(\mathcal{K}^{\Delta t, k} 1)$ denote the changing of mass. We have

$$e^{\mu_{\Delta t}(\lambda)T} = \prod_{k=0}^{M-1} e_k, \quad \text{and} \quad \mu_{\Delta t}(\lambda) = \frac{1}{M\Delta t} \sum_{k=0}^{M-1} \log(e_k). \quad (70)$$

Proof. It is easy to verify that

$$\nu_{\Delta t}^M = \nu_{\Delta t}^0 = \nu_{\Delta t}, \quad (\mathcal{K}^{\Delta t, k})^* \nu_{\Delta t}^k = e_k \nu_{\Delta t}^{k+1}, \quad (71)$$

for some positive numbers e_k 's. These e_k 's are referred to the changing of the mass for each small step $\mathcal{K}^{\Delta t, k}$. Thus, we have $(\mathcal{K}^{\Delta t})^* \nu_{\Delta t}^0 = (\prod_{k=0}^{M-1} e_k) \nu_{\Delta t}^0$, which means $e^{\mu_{\Delta t}(\lambda)T} = \prod_{k=0}^{M-1} e_k$. \square

Finally, we obtain the error estimate of the Lagrangian particle method in computing the principal eigenvalue of parabolic operators as follows.

Theorem 3.11. Let $\xi_k^{p,n-1}$, $k = 1, \dots, M$, $p = 1, \dots, N$, $n \in \mathbb{Z}^+$, and Δt are defined in the N -IPS system Algorithm 1. Then, we have the following convergence result

$$\lim_{N \rightarrow \infty} (M\Delta t)^{-1} \sum_{i=1}^M \log \left(N^{-1} \sum_{p=1}^N \exp(c(t_i, \tilde{\xi}_i^{p,n-1})\Delta t) \right) = \mu(\lambda) + O\left(\left(1 - \frac{\epsilon}{\gamma}\right)^n\right) + O((\Delta t)^{\frac{1}{2}}), \quad (72)$$

where ϵ and γ are defined in Theorem 3.8.

Proof. By the theory of N -IPS system, $\{\xi_k^{p,n-1}\}_{p=1, \dots, N}$ will approximately distributed as $\prod_{i=0}^{k-1} \Phi^{\mathcal{K}^{\Delta t, i}} \Phi_{n-1}^{\mathcal{K}^{\Delta t}} \nu_0$ when $N \rightarrow \infty$. Let $e_{k,n}^N = N^{-1} \sum_{p=1}^N \exp(c(t_k, \tilde{\xi}_k^{p,n-1})\Delta t)$ denote the increasing of the mass for each small step $\mathcal{K}^{\Delta t, k}$. Then, we can get that

$$\lim_{N \rightarrow \infty} e_{k,n}^N = \left(\prod_{i=0}^{k-1} \Phi^{\mathcal{K}^{\Delta t, i}} \Phi_{n-1}^{\mathcal{K}^{\Delta t}} \nu_0 \right) (\mathcal{K}^{\Delta t, k} 1). \quad (73)$$

According to Theorem 3.8, we have that $\Phi_{n-1}^{\mathcal{K}^{\Delta t}} \nu_0 = \nu_{\Delta t} + \delta_n$, where $\|\delta_n\|_{TV} \leq 2\left(1 - \frac{\epsilon}{\gamma}\right)^n$. This implies

$$\lim_{N \rightarrow \infty} e_{k,n}^N = \left(\prod_{i=0}^{k-1} \Phi^{\mathcal{K}^{\Delta t, i}} \nu_{\Delta t} \right) (\mathcal{K}^{\Delta t, k} 1) + O\left(\left(1 - \frac{\epsilon}{\gamma}\right)^n\right). \quad (74)$$

Combining Lemma 3.10, we conclude that

$$\begin{aligned} \lim_{N \rightarrow \infty} (M\Delta t)^{-1} \sum_{i=1}^M \log(e_{k,n}^N) &= (M\Delta t)^{-1} \sum_{k=0}^{M-1} \log(e_k) + O\left(\left(1 - \frac{\epsilon}{\gamma}\right)^n\right) \\ &= \mu_{\Delta t}(\lambda) + O\left(\left(1 - \frac{\epsilon}{\gamma}\right)^n\right). \end{aligned} \quad (75)$$

From Theorem 3.5, we know that $|\mu(\lambda) - \mu_{\Delta t}(\lambda)| = O((\Delta t)^{\frac{1}{2}})$, which concludes the proof. \square

4. Numerical results

In this section, we first present numerical examples to verify the convergence analysis of the proposed method in computing eigenvalues. Then, we compute the KPP front speeds in 2D and 3D chaotic flows. In addition, we investigate the dependence of the KPP front speed on the magnitude of velocity field and the evolution of the empirical distribution of the N -IPS. To be consistent with the setting of numerical experiments in the literature, e.g., [40, 39], we choose the torus space $\mathbb{T}^d = [0, 2\pi]^d$, $d = 2, 3$.

4.1. Convergence tests in computing principal eigenvalue

We first verify the convergence of the operator splitting method in approximating solution operator. Let $\mathbf{x} = (x_1, x_2)^T$. We consider a two-dimensional non-autonomous equation on $[0, 2\pi]^2$ as follows:

$$u_t = \mathcal{L}(t)u + \mathcal{C}(t)u, \quad (76)$$

where $\mathcal{L}(t) = \Delta_{\mathbf{x}} + (\sin(x_2) \cos(2\pi t), \sin(x_1) \cos(2\pi t)) \cdot \nabla_{\mathbf{x}}$ and $\mathcal{C}(t) = (\sin(x_1 + x_2) + \cos(x_1 + x_2)) \sin(2\pi t)$.

We use spectral method to discretize Eq.(76), in order to obtain an accurate approximation in the physical space of the solution operator of Eq.(76). Specially, let $V_H = \text{span}\{e^{i(k_1 x_1 + k_2 x_2)} : -H \leq k_1, k_2 \leq H\}$ denote a finite dimensional space spanned by fourier basis functions, where H is a positive integer. First, we compute the approximations of the operators $\mathcal{L}(t)$ and $\mathcal{C}(t)$ in the space V_H . Let matrices $L^H(t)$ and $C^H(t) \in \mathbb{C}^{(2H+1)^2 \times (2H+1)^2}$ denote the approximations of $\mathcal{L}(t)$ and $\mathcal{C}(t)$, respectively [38]. Then, we use the matrix exponential functions $e^{\Delta t L^H(t)}$ and $e^{\Delta t C^H(t)}$ to approximate $e^{\Delta t \mathcal{L}(t)}$ and $e^{\Delta t \mathcal{C}(t)}$, respectively. Thus, we get an approximation formula for $\mathcal{K}^{\Delta t}$ as

$$K^{H, \Delta t} = \prod_{j=0}^{T/\Delta t - 1} e^{\Delta t L^H(t_j)} e^{\Delta t M^H(t_j)}. \quad (77)$$

For the reference solution, we choose a much finer time step Δt_{ref} and compute the approximation formula

$$\tilde{K}^{H, \Delta t_{ref}} = \prod_{j=0}^{T/\Delta t_{ref} - 1} e^{\Delta t_{ref} (L^H(t_j) + M^H(t_j))}. \quad (78)$$

In this experiment, we choose $H = 24$, $\Delta t = 2^{-1}, 2^{-2}, \dots, 2^{-9}$, and $\Delta t_{ref} = 2^{-12}$. Then, we compute $\|K^{H, \Delta t} - \tilde{K}^{H, \Delta t_{ref}}\|_{L^2}$ to verify our result. Figure 1 shows the convergence results for the splitting method. The convergence rate is $(\Delta t)^{1.05}$. This numerical result suggests that the convergence analysis in Theorem 3.5 is not sharp. More studies on the convergence analysis of our method will be reported in our future work.

Then, we test the convergence of the Lagrangian method, i.e., Algorithm 1, in computing principal eigenvalues of parabolic-type equations. We still consider the problem (76) with the same $\mathcal{L}(t)$ and $\mathcal{C}(t)$. In this experiment, we choose $\Delta t = 2^{-1}, 2^{-2}, 2^{-3}, 2^{-4}, 2^{-5}$, $N = 200,000$ in the N -IPS system, and iteration number $n = 200$ and $n = 400$ in the Feynman-Kac semigroup iteration method. Figure 2 shows the convergence of principal eigenvalues with respect to Δt by spectral method and our Lagrangian method, where the reference solution is computed from spectral method with a finer grid $\Delta t_{ref} = 2^{-10}$. So given sufficient large N and n , the error in calculating principal eigenvalues of linearized KPP operator \mathcal{A} via our proposed Lagrangian approach only comes from the error of operator splitting. Also as the Lagrangian method will eventually converges to some invariant measure approximating the ground truth invariant measure, there is no error accumulation for long time integration.

4.2. Computing KPP front speeds in different flows

We first compute the KPP front speeds in two different time-independent flows, i.e., a 2D steady cellular flow and a 3D ABC flow. Let $\mathbf{x} = (x_1, \dots, x_d)^T \in [0, 2\pi]^d$ with $d = 2, 3$. We use

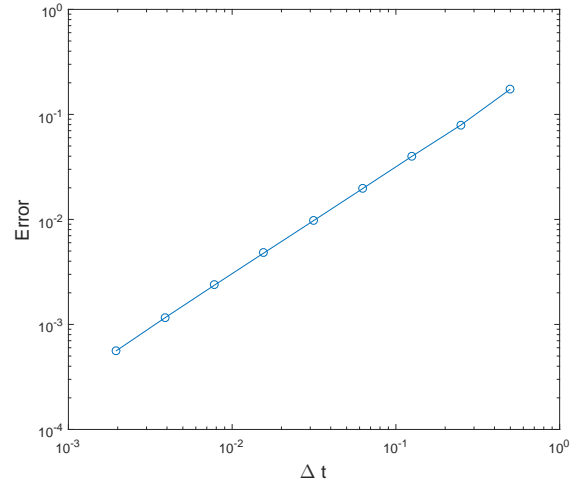


Figure 1: Numerical errors for $\|K^{H,\Delta t} - \tilde{K}^{H,\Delta t_{ref}}\|_{L^2}$.

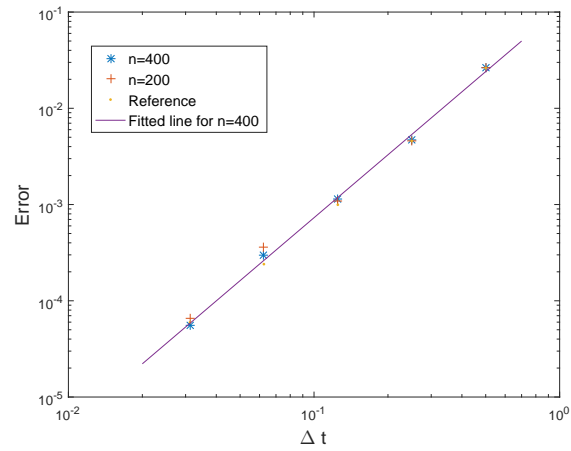


Figure 2: In the Lagrangian method, iteration number $n = 200$ and $n = 400$. The reference solution is obtained by the spectral method.

the Lagrangian method to compute the following principal eigenvalue problem with periodic boundary condition

$$\kappa\Delta_{\mathbf{x}}\Phi + (2\kappa\lambda\mathbf{e} + \mathbf{v}) \cdot \nabla_{\mathbf{x}}\Phi + (\kappa\lambda^2 + \lambda\mathbf{e} \cdot \mathbf{v} + \tau^{-1}f'(0))\Phi = \mu(\lambda)\Phi, \quad (79)$$

$f(u) = u(1-u)$, and $(\mu(\lambda), \Phi)$ are principal eigenvalue of (79) and its associated eigenfunction, respectively. The velocity field $\mathbf{v} = (-\sin x_1 \cos x_2, \cos x_1 \sin x_2)$ in the 2D steady cellular flow and $\mathbf{v} = (\sin x_3 + \cos x_2, \sin x_1 + \cos x_3, \sin x_2 + \cos x_1)$ in the 3D ABC flow, respectively.

We choose the parameters $\kappa = 1$ and $\tau = 1$ in (79). We use the spectral method to obtain an accurate reference solution for the principal eigenvalue of (79). Figure 3 shows the convergence results of the Lagrangian method in computing the principal eigenvalue, where $\lambda = 0.35$ for the 2D cellular flow and $\lambda = 0.55$ for the 3D ABC flow. We find the convergence rate of the Lagrangian method is $(\Delta t)^{1.51}$ for the 2D steady cellular flow, and $(\Delta t)^{1.70}$ for the 3D ABC flow. Thus, we can use the Lagrangian method to compute the KPP front speeds in both 2D and 3D flows.

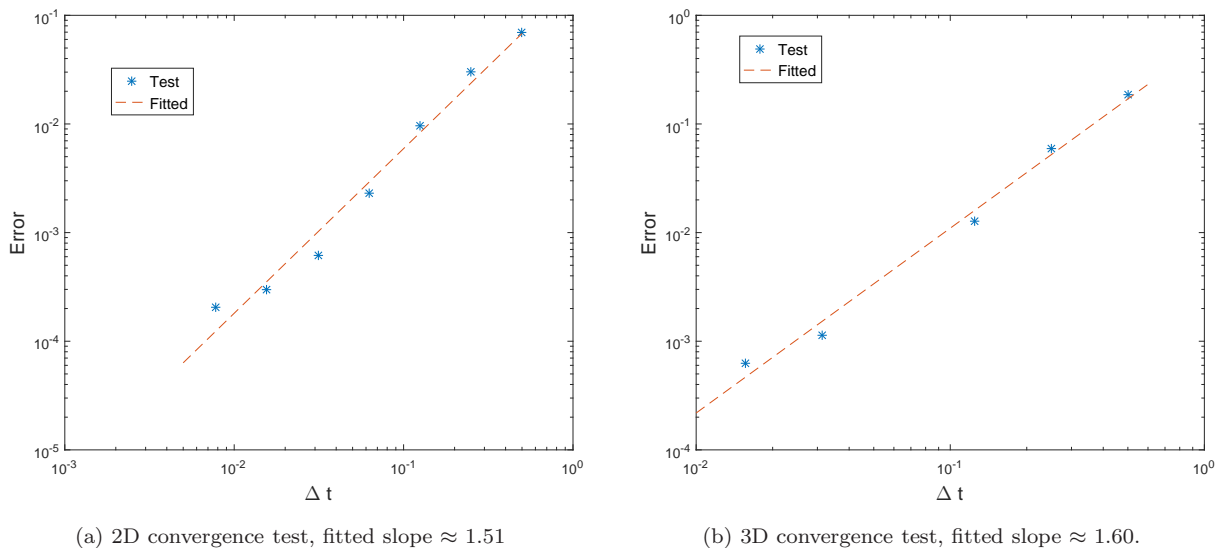


Figure 3: Errors of the principal eigenvalue computed by using different time steps.

After getting the principal eigenvalue, we compute the KPP front speed c^* through the formula $c^* = \inf_{\lambda > 0} \frac{\mu(\lambda)}{\lambda}$. We only show the numerical results for the 3D ABC flow here since the results for the 2D steady cellular flow is quantitatively similar. We choose the velocity field $\mathbf{v} = A(\sin x_3 + \cos x_2, \sin x_1 + \cos x_3, \sin x_2 + \cos x_1)$, where A is the strength of the convection. In Figure 4, we show the results of $\frac{\mu(\lambda)}{\lambda}$ for ABC flows with $A = 1$ and $A = 10$. The amplitude of the principal eigenvalue increases fast and the convergence speed becomes slower. Notice that in this case, the flow becomes very unstable since the convection becomes dominant comparing to the diffusion. This issue will be studied in subsection 4.3.

Next, we compute the KPP front speed in a 2D unsteady (time-dependent) cellular flow. Let $\mathbf{x} = (x_1, x_2)^T$. We use the Lagrangian method to compute the following principal eigenvalue problem with periodic boundary condition

$$\kappa\Delta_{\mathbf{x}}\Phi + (2\kappa\lambda\mathbf{e} + \mathbf{v}) \cdot \nabla_{\mathbf{x}}\Phi + (\kappa\lambda^2 + \lambda\mathbf{e} \cdot \mathbf{v} + \tau^{-1}f'(0))\Phi - \Phi_t = \mu(\lambda)\Phi, \quad (80)$$

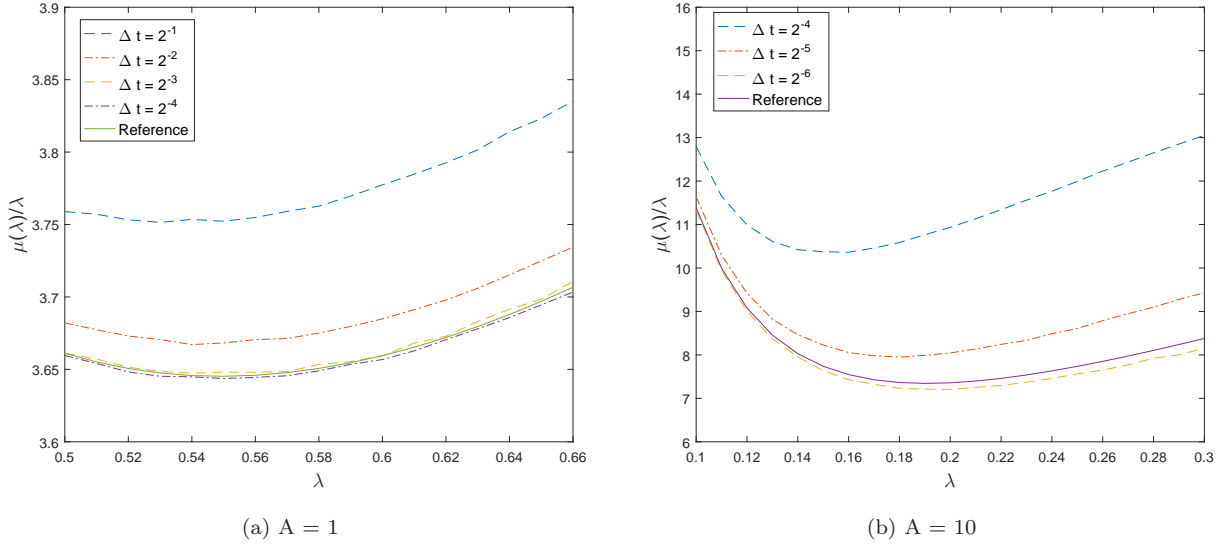


Figure 4: Numerical results of $\frac{\mu(\lambda)}{\lambda}$ for different λ 's in the ABC flow.

where $(t, \mathbf{x}) \in [0, T] \times [0, 2\pi]^2$, T is the period of \mathbf{v} in t , $f(u) = u(1 - u)$, and $(\mu(\lambda), \Phi)$ are principal eigenvalue of (80) and its associated eigenfunction, respectively. The velocity field of the 2D unsteady cellular flow is $\mathbf{v} = (-\sin x_1 \cos x_2(1 + \delta \cos 2\pi t), \cos x_1 \sin x_2(1 + \delta \cos 2\pi t))$, where $\delta > 0$ is a parameter.

We choose the parameters $\kappa = 1$ and $\tau = 1$ in (80) and $\delta = 0.5$ in the velocity field \mathbf{v} . We use the spectral method to obtain an accurate reference solution for the principal eigenvalue of (80). For figure 5a, we choose $\lambda = 0.57$. Figure 5a shows the convergence results of the Lagrangian method in computing the principal eigenvalue, where the convergence rate is $(\Delta t)^{1.31}$. Figure 5b shows the numerical results of $\frac{\mu(\lambda)}{\lambda}$ for different λ 's, from which we can compute the KPP front speed in the 2D unsteady cellular flow. We can see that $\frac{\mu(\lambda)}{\lambda}$ is convex within the computational domain of λ . Thus, we can compute the KPP front speed by finding the minimizer of $\frac{\mu(\lambda)}{\lambda}$.

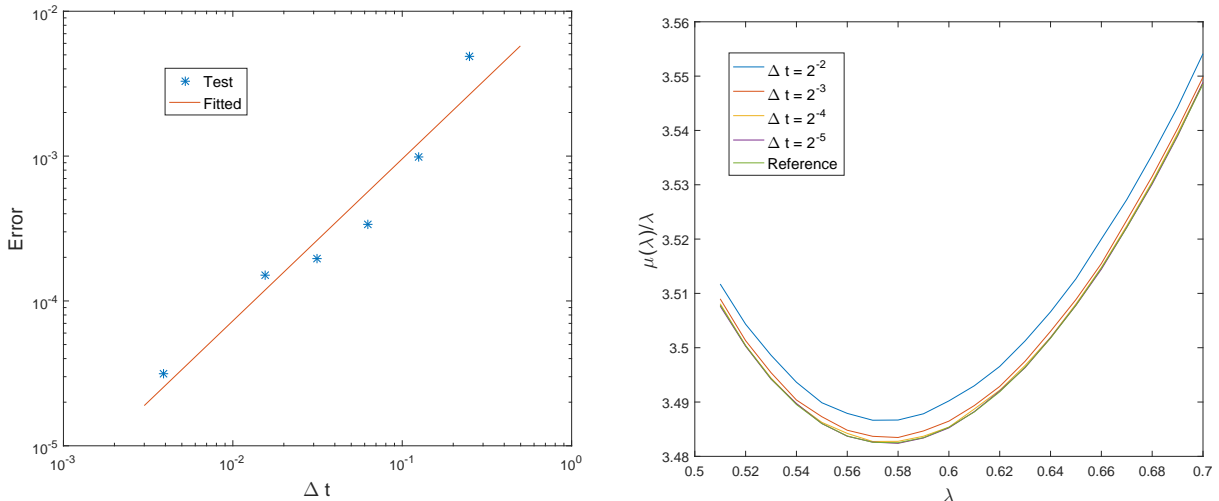
4.3. Investigate the dependence of front speed on the strength of the flows

To further test the performance of the Lagrangian method, we study the dependence of the KPP front speeds on the strength of different flows. Moreover, we study the relationship between the KPP front speeds in the chaotic flows and the effective diffusivity of the passive tracer model in the same chaotic flows. We refer the interested reader to [43, 42, 23] for the recent development in computing effective diffusivities in chaotic and random flows. We set the diffusion constant $\kappa = 1$ and the time scale of reaction rate $\tau = 1$.

Let us first consider this issue in KPP front speeds of time-independent flows. If we scale $\mathbf{v} \rightarrow A\mathbf{v}$, Eq.(79) can be rewritten as the following form

$$\Delta_{\mathbf{x}}\Phi + (2\lambda\mathbf{e} + A\mathbf{v}) \cdot \nabla_{\mathbf{x}}\Phi + (\lambda^2 + \lambda\mathbf{e} \cdot A\mathbf{v} + f'(0))\Phi = \mu(\lambda)\Phi. \quad (81)$$

The KPP front speed is $c^* = \inf_{\lambda>0} \frac{\mu(\lambda)}{\lambda}$. Notice that the KPP front speed c^* depends on A ,



(a) Convergence test for different Δt 's. The fitted slope is ≈ 1.31 .

(b) Numerical results of $\frac{\mu(\lambda)}{\lambda}$ for different λ 's.

Figure 5: Numerical results for a 2D unsteady cellular flow.

i.e., $c^* = c^*(A)$. Therefore, we consider the equivalent equation

$$A^{-1}\Delta_{\mathbf{x}}\Phi + (2A^{-1}\lambda\mathbf{e} + \mathbf{v}) \cdot \nabla_{\mathbf{x}}\Phi + (A^{-1}\lambda^2 + \lambda\mathbf{e} \cdot \mathbf{v} + A^{-1}f'(0))\Phi = \tilde{\mu}(\lambda)\Phi, \quad (82)$$

where $\tilde{\mu}(\lambda) = A^{-1}\mu(\lambda)$. Let \tilde{c}^* denote the KPP front speed of the rescaled equation (82). We have that

$$\tilde{c}^* = \inf_{\lambda > 0} \frac{\tilde{\mu}(\lambda)}{\lambda} = \frac{c^*}{A}. \quad (83)$$

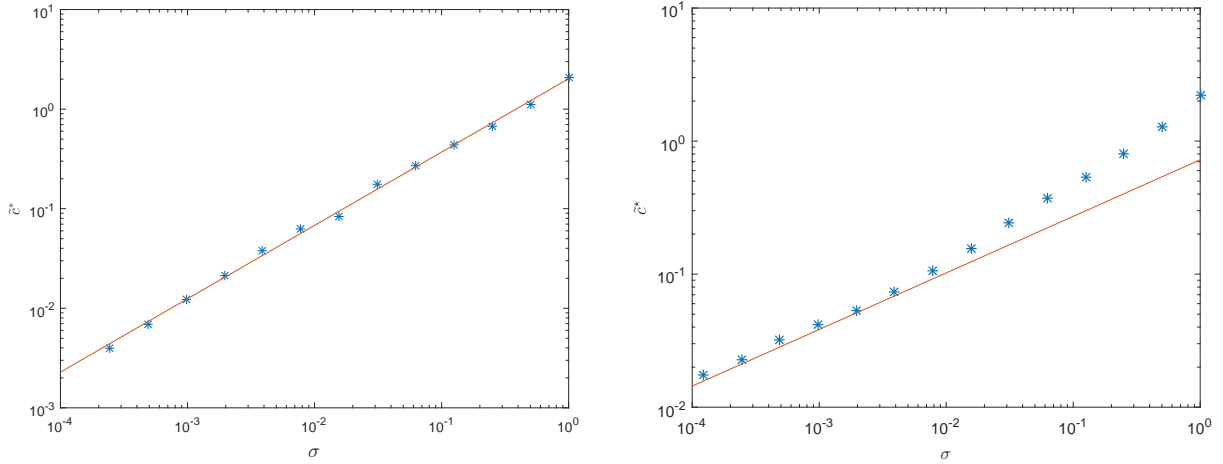
We denote $\sigma = A^{-1}$. For the 2D steady cellular flow $\mathbf{v} = (-\sin x_1 \cos x_2, \cos x_1 \sin x_2)$, it has been proved that $c^*(A) = O(A^{1/4})$ [1, 34]. Let $D^E(A)$ denote the effective diffusivity corresponding of the passive tracer model in the same 2D steady cellular flow \mathbf{v} . It has been proved by a boundary layer analysis that $D^E(A) = O(A^{1/2})$ in [1, 6]. By scaling analysis, we obtain that for the 2D steady cellular flow the following result holds

$$c^*(A) = O(\sqrt{D^E(A)}). \quad (84)$$

To the best of our knowledge, the above relationship between the KPP front speeds and the effective diffusivity was only proved in 2D steady cellular flows; see [34, 36]. The result (84) implies that $\tilde{c}^*(\sigma) = \sigma O(\sigma^{-1/4}) = O(\sigma^{3/4})$, which provides a theoretical guidance for our numerical experiments. Figure 6a shows the numerical results of $\tilde{c}^*(\sigma)$ in the 2D steady cellular flow obtained by our method. From the numerical results, we compute regression and obtain $\tilde{c}^*(\sigma) = O(\sigma^{0.74})$, which agrees with the theoretical result (84).

For other flows, such as unsteady flows and 3D chaotic flows, the understanding of $c^*(A)$ for large A 's (or $\tilde{c}^*(\sigma)$ for small σ 's) remains open. We will study these flows here. In our previous work [42], we computed the effective diffusivity of the passive tracer model in the 3D Kolmogorov flow, where $\mathbf{v} = (\sin x_1, \sin x_2, \sin x_3)$, and obtained that $D^E(A) = O(A^{1.13})$. Notice that in [42] the effective diffusivity is represented in terms of the diffusion and we have

converted the result in terms of the strength of the flows here, which are equivalent. The result (84) implies that $\tilde{c}^*(\sigma) = \sigma O(\sigma^{-0.56}) = O(\sigma^{0.44})$. Using our method, we compute $\tilde{c}^*(\sigma)$ for σ in 3D Kolmogorov flow and show the numerical results in Figure 6b. We obtain that $\tilde{c}^*(\sigma) = O(\sigma^{0.43})$, which means that the result (84) also holds in the 3D Kolmogorov flow. We conjecture that the result (84) also holds true in other 3D chaotic flows. We will study this issue in future works.



(a) Numerical results of $\tilde{c}^*(\sigma)$ in 2D cellular flow. The fitted slope is ≈ 0.74 . (b) Numerical results of $\tilde{c}^*(\sigma)$ in 3D Kolmogorov flow. The fitted slope is ≈ 0.43 .

Figure 6: Numerical results of $\tilde{c}^*(\sigma)$ in different flows.

Next, we study the dependence of the KPP front speeds on the strength of time-dependent flows. Specifically, we will consider two 3D flows. The first one is a time-dependent Kolmogorov flow with $\mathbf{v} = (\sin(x_3 + \theta \sin(2\pi t)), \sin(x_1 + \theta \sin(2\pi t)), \sin(x_2 + \theta \sin(2\pi t)))$, and the second one is a time-dependent ABC flow with $\mathbf{v} = (\sin(x_3 + \sin(2\pi\Omega t)) + \cos(x_2 + \sin(2\pi\Omega t)), \sin(x_1 + \sin(2\pi\Omega t)) + \cos(x_3 + \sin(2\pi\Omega t)), \sin(x_2 + \sin(2\pi\Omega t)) + \cos(x_1 + \sin(2\pi\Omega t)))$.

For the 3D time-dependent Kolmogorov flow, we choose iteration time $n = 256$, time step $\Delta t = 2^{-9}$ and particle number $N = 400,000$. Figure 7 shows the result of $\tilde{c}^*(\sigma)$ for small σ 's and different θ 's. Again, we find the KPP front speed $\tilde{c}^*(\sigma)$ is not very sensitive to the parameter θ . When $\theta = 1$, we obtain that $\tilde{c}^*(\sigma) = O(\sigma^{0.39})$.

In Figure 8, we plot out procedure searching for the λ when the minimal in Eq.(83) was reached. We use $a\lambda + b\lambda^{-1} + c$ to fit a curve, then find the minimum of the curve. When σ is large, the relative fluctuation is small and the minimum is easily to be find. When σ is small, the relative fluctuation becomes strong enough, so we decide to fit the curve, then find the minimum point.

For the 3D time-dependent ABC flow, we choose the iteration time $n = 2048$ (since the ABC flow is more chaotic), time step $\Delta t = 2^{-9}$, and particle number $N = 400,000$. Figure 9a shows the KPP front speeds $\tilde{c}^*(\sigma)$ for different Ω 's, where Ω ranges from 2^{-7} to 2^0 . Figure 9b shows the slope of each approximation line for each Ω in Figure 9a. If we assume $\tilde{c}^*(\sigma) = O(\sigma^\alpha)$ is true, the slope values in Figure 9b give the power value α 's for different Ω 's. We find that when Ω is near 0.1, the power value α is large. When Ω is away from 0.1, say $\Omega < 2^{-4}$ or

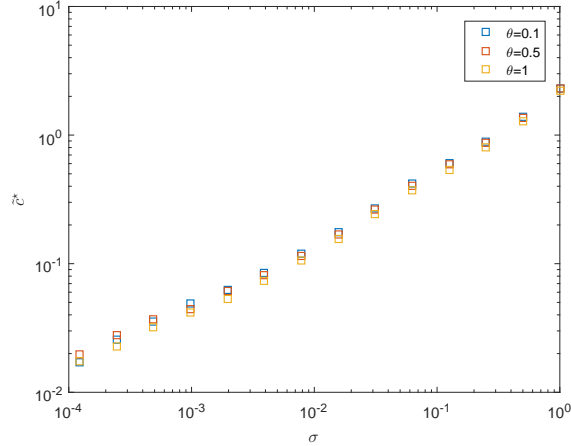


Figure 7: Numerical results of $\tilde{c}^*(\sigma)$ in a 3D time-dependent Kolmogorov flow.

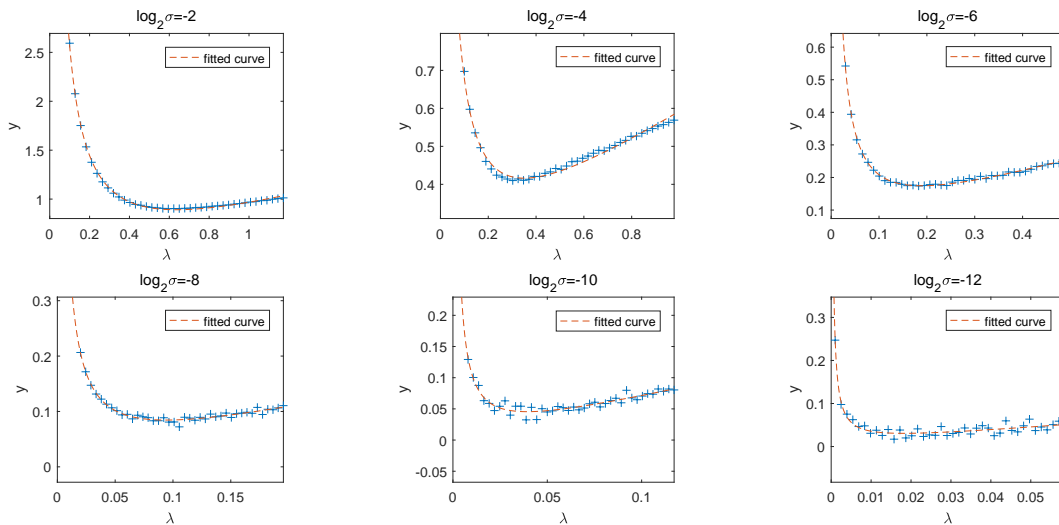
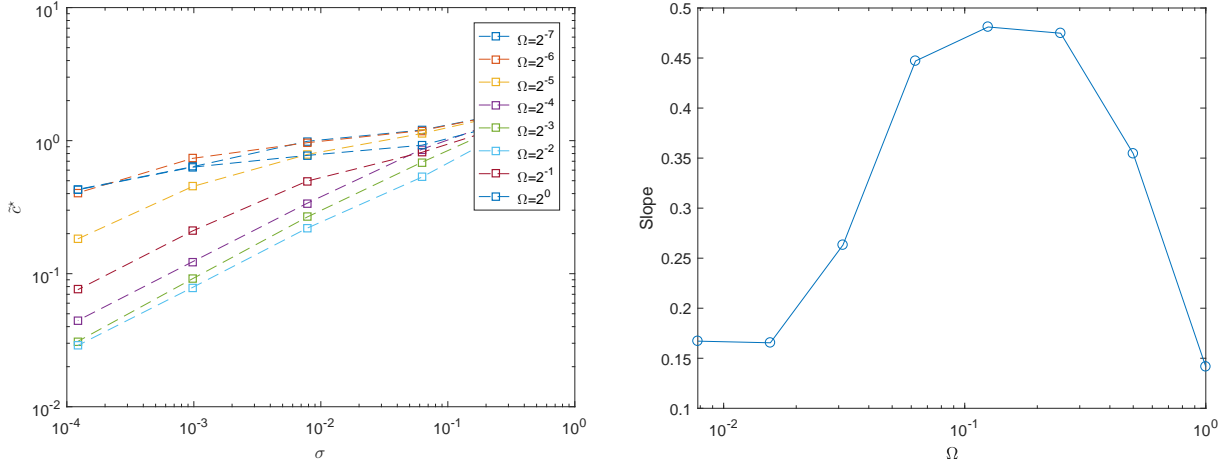


Figure 8: Numerical results of $\frac{\mu(\lambda)}{\lambda}$ for different λ 's and σ 's in the 3D time-dependent Kolmogorov flow. The red dash curve is fitted by $a\lambda + b\lambda^{-1} + c$.

$\Omega > 2^{-2}$, the power value α is small. A similar sensitive dependence on the frequency of time-dependent ABC flows was reported in [4], where the Lyapunov exponent of the deterministic time-dependent ABC flow problem (i.e., $\Omega = 0$) was studied as the indicator of the extent of chaos; see Figure 2 and Figure 3 of [4].

We compare the computational time of the interacting particle method and the spectral method in the 2D cellular flow example. The numerical experiments are carried out on the same core of the HPC2015 system at HKU with 10-core Intel Xeon E5-2600 v3(Haswell) processors and 96 GB physical memory. We compute the front speed using the spectral method mentioned in Section 4.1. We set the Fourier modes $H = 2^k$ and k is a positive integer. When $\sigma = 2^{-2}$, for the spectral method, $H = 2^3$ is enough and it spends 1.13 seconds to calculate the front speed; while for our interacting particle method, the computational time is about 45.01 seconds. When $\sigma = 2^{-5}$, for the spectral method, $H = 2^4$ is enough



(a) Numerical results of $\tilde{c}^*(\sigma)$ for different Ω 's and different σ 's. (b) Power values of $\tilde{c}^*(\sigma) = O(\sigma^\alpha)$ for different Ω 's.

Figure 9: Numerical results for the time-dependent ABC flows.

and it spends 42.35 seconds to calculate the front speed, and the interacting particle method costs 172.76 seconds. When $\sigma = 2^{-8}$, for the spectral method, $H = 2^4$ is needed and it costs 1203.12 seconds to calculate the front speed; on the other hand, our interacting particle method costs 676.23 seconds. When σ becomes extremely small, the spectral method becomes very expensive, however, our interacting particle method is still very efficient. For instance, when $\sigma = 2^{-12}$, the spectral method may need several days to calculate the front speed, but our interacting particle method only costs 5378.24 seconds. We remark that the spectral method becomes very expensive in computing front speeds for 3D chaotic flows. However, the computational time of the interacting particle method only weakly depends on the dimension of the physical space. Thus, we can compute KPP front speeds in 3D chaotic flows.

4.4. Evolution of the empirical distribution of the particles

As stated in Theorem 3.8, the empirical distribution converges to the invariant measure of Feynman-Kac semigroup as n approaches infinity. Our Lagrangian method can not only calculate the principal eigenvalue but also compute the evolution of the distribution. In this subsection, we will study the empirical distribution of the N -IPS system moduled to torus space. In this subsection, the particle number for all tests is $N = 200,000$.

Figure 10 shows the invariant distribution generated by the N -IPS system in the 2D steady cellular flow, where $\mathbf{v} = (-\sin x_1 \cos x_2, \cos x_1 \sin x_2)$. The parameter σ varies from 2^0 to 2^{-5} . The strength of the convection is then proportion to $1/\sigma$. Then we can see from the graph when increasing the strength, the main part of invariant measure gets into a smaller domain and the gradient becomes sharper, which is a common phenomenon in fluid dynamics. In addition, by comparing to the pattern at the boundary of the plot, one can find that the invariant measure is periodic in physical space.

Next, we study the evolution of invariant distribution generated by our N -IPS system in a 2D time-periodic mixing flow, where $\mathbf{v} = (-\cos x_2 - \theta \sin x_1 \cos(2\pi t), \cos x_1 + \theta \sin x_2 \cos(2\pi t))$. Figure 11 shows the empirical distribution of the N -IPS system at different times within one

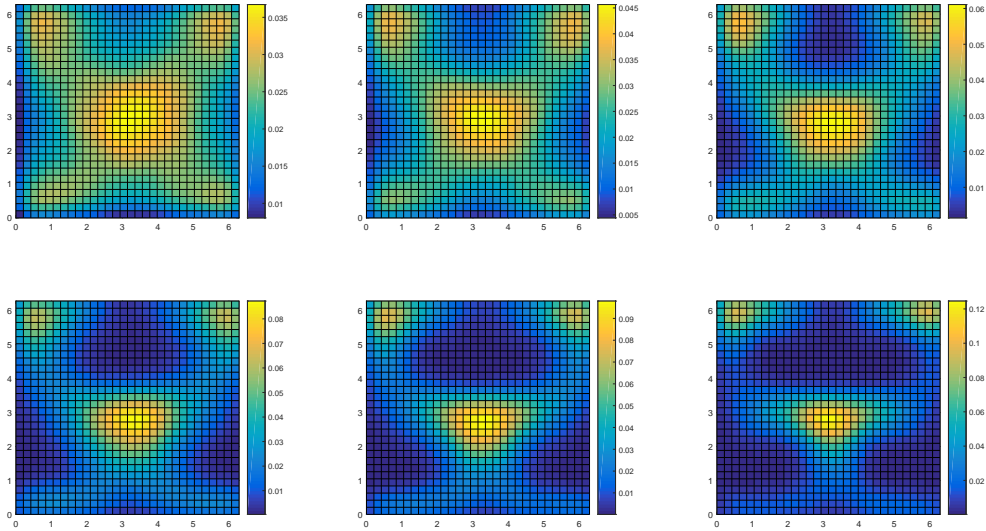


Figure 10: Empirical distributions for the 2D steady cellular flow with σ varies from 2^0 to 2^{-5} . First row from left to right: $\sigma = 2^0$, $\sigma = 2^{-1}$, and $\sigma = 2^{-2}$. Second row from left to right: $\sigma = 2^{-3}$, $\sigma = 2^{-4}$, and $\sigma = 2^{-5}$.

period when the iteration time $n = 400$. From these numerical results, we can see the invariant distribution varies at different times of one period. But as the starting time of different periods, the first and last subfigure are identical. These are consistent with our expectation obtained in Lemma 3.10, where we proved that the invariant measure changes periodically with the same period as the flow.

Finally, we let the parameter σ vary from 2^0 to 2^{-5} and study the evolution of invariant distribution generated by our N -IPS system in the 2D time-periodic mixing flow. Figure 12 shows that with the increasing of the strength of the convection, the invariant measure becomes compactly supported with a sharp gradient.

From these numerical results, we get two conclusions. First, the invariant measure of the Feynman-Kac semigroup associated with the KPP operator is no longer uniform distribution. This is due to the effect from the potential function $c(t, \mathbf{x})$. Second, the invariant measure converges to a limiting measure as $\sigma \rightarrow 0$. Notice that when σ is small, the invariant measure develops sharp gradients, which requires more particles to compute. Moreover, it may take more iteration time steps to converges. Developing effective sampling method to compute invariant measure for the KPP operator with small diffusion constant will be studied in our future works.

5. Conclusion

In this paper, we developed efficient Lagrangian particle methods to compute the KPP front speeds in time-periodic cellular and chaotic flows and provided rigorous convergence analysis for the numerical schemes. In the convergence analysis, we first obtained the error of the operator splitting methods in approximating the solution operator corresponding to the linearized KPP equation. Then, we proved the convergence of the Lagrangian particle method

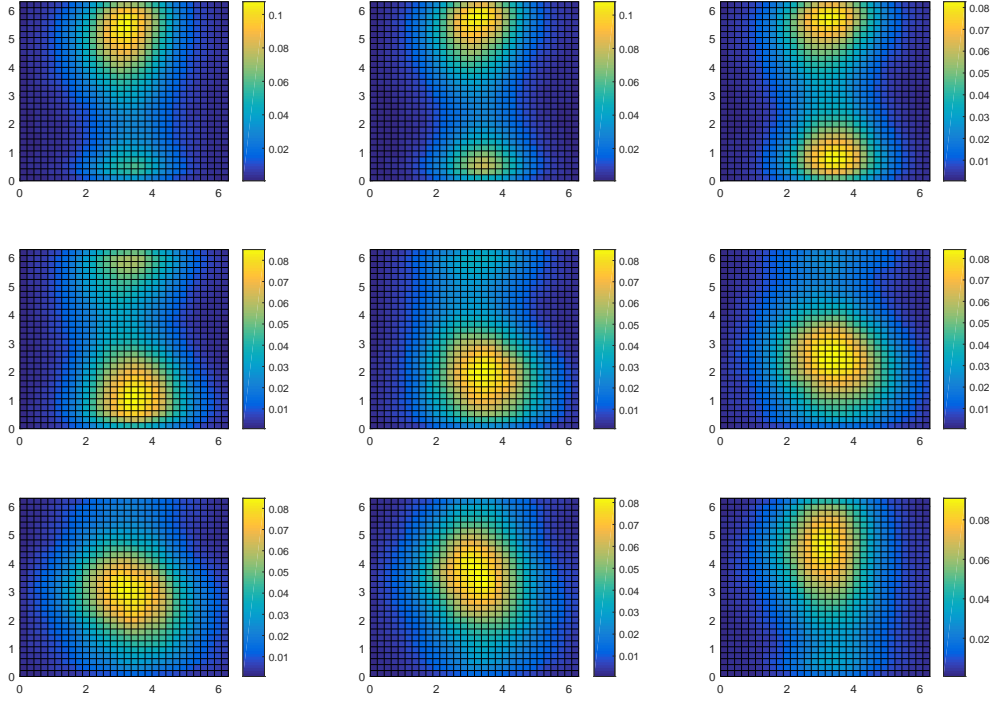


Figure 11: Empirical distributions for the 2D time-periodic mixing flow with $\theta = 1$, $\sigma = 1$, in different phase of one period: t varies from 0 to 1 with time interval equal to $1/9$.

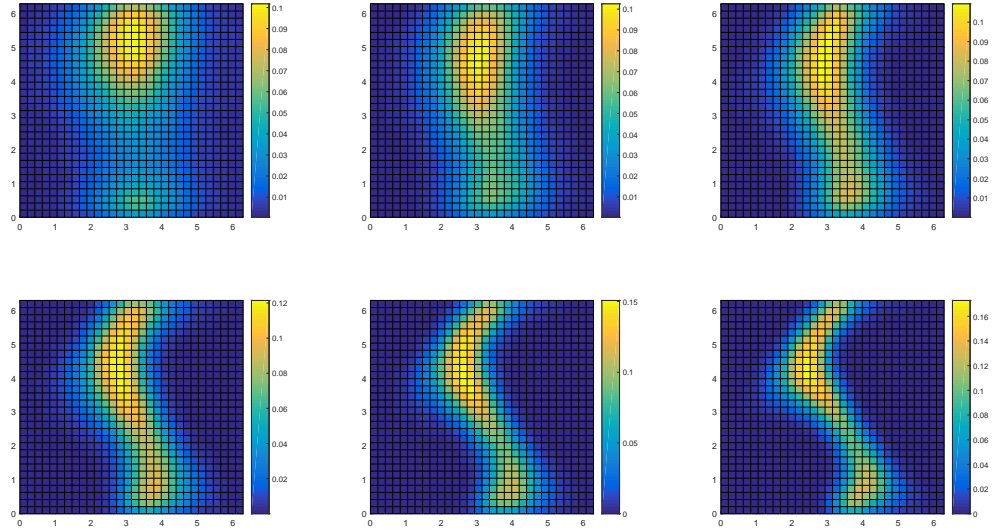


Figure 12: Empirical distributions for the 2D time-periodic mixing flow with $\theta = 1$, σ varies from 2^0 to 2^{-5} . First row from left to right: $\sigma = 2^0$, $\sigma = 2^{-1}$, and $\sigma = 2^{-2}$. Second row from left to right: $\sigma = 2^{-3}$, $\sigma = 2^{-4}$, and $\sigma = 2^{-5}$.

in computing the principal eigenvalue based on the Feynman-Kac semigroup theory. Finally, we presented numerical results to verify the convergence rate of the proposed method for computing the principal eigenvalues. In addition, we computed the KPP front speeds in several typical chaotic flow problems of physical interests, including the Arnold-Beltrami-Childress (ABC) flow and the Kolmogorov flow. It has been proved that the KPP front speed and the effective diffusivity satisfies the relation $c^*(A) = O(\sqrt{D^E(A)})$ in 2D cellular flows [34, 36]. We numerically verified this relation and found that this relation still holds in 3D Kolmogorov flows and ABC flows.

There are three directions we plan to explore in our future work. First, we will extend the Lagrangian particle method to compute KPP front speeds in time-stochastic and space-periodic flows. Second, we will develop Lagrangian particle methods to compute KPP front speeds in more complex fluid flows, where the computational domain is not compact. This type of problem is more challenging both analytically and numerically. As stated in the introduction part, there is limited literature on studying the existence of KPP front speeds in complex flows. In the aspect of numerical computation, our current method cannot be adapted to non-compact domains. We shall adopt some relaxation techniques to address this problem. In addition, we shall develop adaptive sampling methods for our Lagrangian particle methods in order to resolve the sharp gradients in the invariant measure when the magnitude of the velocity field is very large.

Acknowledgement

The research of J. Lyu and Z. Wang are partially supported by the Hong Kong PhD Fellowship Scheme. The research of J. Xin is partially supported by NSF grants DMS-1924548 and DMS-1952644. The research of Z. Zhang is supported by Hong Kong RGC grants (Projects 17300817 and 17300318), Seed Funding Programme for Basic Research (HKU), and Basic Research Programme (JCYJ20180307151603959) of The Science, Technology and Innovation Commission of Shenzhen Municipality. The computations were performed using the HKU ITS research computing facilities that are supported in part by the Hong Kong UGC Special Equipment Grant (SEG HKU09).

Appendix A. Error bounds for exponential operator splitting in non-autonomous evolution equations

Appendix A.1. Euler methods for non-autonomous evolution equations

In this section, we review the fundamental results for abstract linear evolution equations by semigroup theory; see e.g. [11, 5] for more details. We consider the non-autonomous Cauchy problem (NCP) as follows

$$\begin{cases} \frac{d}{dt}u(t) = \mathcal{A}(t)u(t), & t \geq s \in \mathbb{R} \\ u(s) = x \in X, \end{cases} \quad (\text{A.1})$$

where X is a Banach space and $(\mathcal{A}(t), \mathcal{D}(\mathcal{A}(t)))_{t \in \mathbb{R}}$ is a family of linear operators on X .

Definition Appendix A.1. A continuous function $u : [s, \infty) \rightarrow X$ is called a classical solution of (A.1) if $u \in C^1([s, \infty); X)$, $u(t) \in \mathcal{D}(\mathcal{A}(t))$ for all $t \geq s$, $u(s) = x$, and $\frac{d}{dt}u(t) = \mathcal{A}(t)u(t)$ for all $t \geq s$.

Definition Appendix A.2. For a family $(\mathcal{A}(t), \mathcal{D}(\mathcal{A}(t)))_{t \in \mathbb{R}}$ of linear operators on a Banach space X , the NCP (A.1) is well-posed with regularity subspace $(Y_s)_{s \in \mathbb{R}}$ and exponentially bounded solutions, if

(i) (Existence) For all $s \in \mathbb{R}$ the subspace

$$Y_s = \{y \in X : \text{there exists a classical solution for the NCP (A.1)}\} \subset \mathcal{D}(\mathcal{A}(s)) \quad (\text{A.2})$$

is dense in X .

(ii) (Uniqueness) For every $y \in Y_s$, the solution $u_s(\cdot, y)$ is unique.

(iii) (Continuous dependence) The solution continuously depends on s and y , i.e., if $s_n \rightarrow s \in \mathbb{R}$, $\|y_n - y\|_X \rightarrow 0$ with $y_n \in Y_{s_n}$, then we have $\|\hat{u}_{s_n}(t, y_n) - \hat{u}_s(t, y)\|_X \rightarrow 0$ uniformly for t in compact subsets of \mathbb{R} , where

$$\hat{u}_s(t, y) = \begin{cases} u_r(t, y) & \text{if } r \leq t, \\ y & \text{if } r > t. \end{cases}$$

(iv) (Exponential boundedness) There exists a constant $\omega \in \mathbb{R}$ such that

$$\|u_s(t, y)\|_X \leq e^{\omega(t-s)} \|y\|_X$$

for all $y \in Y_s$ and $t \geq s$.

Definition Appendix A.3. A family $\{\mathcal{U}(t, s), t \geq s\}$ of linear, bounded solution operators on Banach space X is called an exponentially bounded evolution family if

- (i) $\mathcal{U}(t, r)\mathcal{U}(r, s) = \mathcal{U}(t, s)$ and $\mathcal{U}(t, t) = Id$ hold for all $t \geq r \geq s \in \mathbb{R}$,
- (ii) the mapping $(t, s) \rightarrow \mathcal{U}(t, s)$ is strongly continuous,
- (iii) $\|\mathcal{U}(t, s)\|_X \leq e^{\omega(t-s)}$ for some $\omega \in \mathbb{R}$ and all $t \geq s \in \mathbb{R}$.

In contrast to the behavior of C_0 -semigroups, the algebraic proposition of an evolution family do not imply any differentiability on a dense subspace. Therefore, we need extra assumptions in order to solve an NCP.

Definition Appendix A.4. An evolution family $\{\mathcal{U}(t, s), t \geq s\}$ is called evolution family solving NCP (A.1) if for every $s \in \mathbb{R}$ the regularity space

$$Y_s = \{y \in X : [s, \infty) \ni t \mapsto \mathcal{U}(t, s)y \text{ solves NCP (A.1)}\}$$

is dense in X .

In this case, the unique classical solution of the NCP (A.1) is given by $u(t) = \mathcal{U}(t, s)x$. The well-posedness of the NCP (A.1) can now be characterized by the existence of solving an evolution family $\{\mathcal{U}(t, s), t \geq s\}$.

Proposition Appendix A.5. Let X be a Banach space and $(\mathcal{A}(t), \mathcal{D}(\mathcal{A}(t)))_{t \in \mathbb{R}}$ be a family of linear operators on X . The following assertions are equivalent [11].

- (i) The NCP (A.1) is well-posed.
- (ii) There exists a unique evolution family $\{\mathcal{U}(t, s), t \geq s\}$ solving the NCP (A.1).

In addition, if $\|e^{\tau \mathcal{A}(t)}\|_X \leq e^{\omega \tau}$ for any $\tau \geq 0, t \in \mathbb{R}$, then we have $\|\mathcal{U}(t, s)\|_X \leq e^{\omega(t-s)}$.

The well-posedness of non-autonomous evolution equations is complicated and there is no general theory describing it. Conditions implying well-posedness are generally divided into parabolic-type assumptions and hyperbolic-type ones. Due to the property of the KPP equation, we only study the parabolic-type conditions in this paper, where the domain $(\mathcal{D}(\mathcal{A}(t)))$ is independent of $t \in \mathbb{R}$. We refer the interested reader to [37] for more general cases.

Assumption Appendix A.6. (Parabolic-type conditions)

- (P1) The domain $\mathcal{D} = \mathcal{D}(\mathcal{A}(t))$ is independent of $t \in \mathbb{R}$.
- (P2) For each $t \in \mathbb{R}$ the operator $\mathcal{A}(t)$ is sectorial and generates an analytic semigroup $e^{\cdot \mathcal{A}(t)}$. For all $t \in \mathbb{R}$, the resolvent $\mathcal{R}(\gamma_1, \mathcal{A}(t))$ exists for all $\gamma_1 \in \mathbb{C}$ with $\text{Re} \gamma_1 \geq 0$ and there is a constant $M \geq 1$ such that

$$\|\mathcal{R}(\gamma_1, \mathcal{A}(t))\|_X \leq \frac{M}{|\gamma_1| + 1} \quad (\text{A.3})$$

for $\text{Re} \gamma_1 \geq 0$ and $t \in \mathbb{R}$. The semigroups $e^{\cdot \mathcal{A}(t)}$ satisfy $\|e^{\tau \mathcal{A}(t)}\|_X \leq e^{\omega \tau}$ for some constant $\omega \in \mathbb{R}$.

- (P3) There exist constants $L \geq 0$ and $0 < \theta \leq 1$ such that

$$\|(\mathcal{A}(t) - \mathcal{A}(s))\mathcal{A}(0)^{-1}\|_X \leq L|t - s|^\theta, \text{ for all } t, s \in \mathbb{R}. \quad (\text{A.4})$$

To obtain a convergence estimate for the operator in certain norm, we need an additional assumption on $\mathcal{A}(t)$ as follows.

Assumption Appendix A.7. The operator $\mathcal{A}(t)$ satisfies a Hölder continuous condition. Namely, there exists $0 \leq \alpha < \beta$ such that for any $x \in \mathcal{D}(\mathcal{A})$,

$$\|(\mathcal{A}(t) - \mathcal{A}(s))x\|_X \leq C|t - s|^\beta \|\mathcal{A}(\tau)x\|_X^\alpha \|x\|_X^{1-\alpha}, \quad (\text{A.5})$$

for any $s \leq \tau \leq t$.

For forward Euler type discretization, Assumption Appendix A.7 can be relaxed to $\tau = s$ only. The backward Euler type discretization needs $\tau = t$, and other discretization methods need different τ 's instead. For analytic semigroups, the following estimate holds true [11, 35].

Lemma Appendix A.8. Let $e^{t\mathcal{A}}$ be an analytical semigroup on X . Let \mathcal{A} be the infinitesimal generator. There is a constant $C \geq 0$ such that

$$\|\mathcal{A}e^{t\mathcal{A}}\|_X \leq \frac{C}{t}, \quad t > 0, \quad 0 \leq \alpha \leq 1. \quad (\text{A.6})$$

Now we state the first result, which gives the approximation error of the freezing time coefficients methods for solving the NCP (A.1).

Theorem Appendix A.9. Suppose assumptions Appendix A.6 and Appendix A.7 hold true. Let $\mathcal{U}(T, 0)$ be the solution operator associated with the NCP (A.1). Then the solution operator obtained by the freezing time coefficients methods has the following approximation error to $\mathcal{U}(T, 0)$

$$\left\| \mathcal{U}(T, 0) - \prod_{k=0}^{M-1} e^{\Delta t \mathcal{A}(k\Delta t)} \right\|_X \leq C(T)(\Delta t)^{\beta-\alpha}, \quad (\text{A.7})$$

where $T > 0$, M is an integer, and $\Delta t = \frac{T}{M}$.

Proof. First we refer to [37] for the abstract version of the method of freezing coefficients,

$$\mathcal{U}(t, s) = e^{(t-s)\mathcal{A}(s)} + \int_s^t \mathcal{U}(t, \tau)(\mathcal{A}(\tau) - \mathcal{A}(s))e^{(\tau-s)\mathcal{A}(s)} d\tau \quad (\text{A.8})$$

which immediately gives us that, for every $x \in X$,

$$\begin{aligned} & \left\| (\mathcal{U}(t, s) - e^{(t-s)\mathcal{A}(s)})x \right\|_X \\ &= \left\| \int_s^t \mathcal{U}(t, \tau)(\mathcal{A}(\tau) - \mathcal{A}(s))e^{(\tau-s)\mathcal{A}(s)}x d\tau \right\|_X \\ &\leq \int_s^t \left\| \mathcal{U}(t, \tau) \right\|_X (\tau - s)^\beta \left\| \mathcal{A}(s)e^{(\tau-s)\mathcal{A}(s)}x \right\|_X^\alpha \left\| e^{(\tau-s)\mathcal{A}(s)}x \right\|_X^{1-\alpha} d\tau. \end{aligned} \quad (\text{A.9})$$

In (A.9), we have used the fact that $e^{(\tau-s)\mathcal{A}(s)}x \in \mathcal{D}(\mathcal{A})$ for any $x \in X$. Notice that $\mathcal{A}(s)$ generates an analytic semigroup $e^{\mathcal{A}(s)}$, according to (Appendix A.8) we have the following estimate

$$\left\| \mathcal{A}(s)e^{(\tau-s)\mathcal{A}(s)} \right\|_X^\alpha \leq C(\tau - s)^{-\alpha} e^{\omega\alpha(\tau-s)}. \quad (\text{A.10})$$

Substituting (A.10) into (A.9), we obtain that,

$$\begin{aligned} & \left\| (\mathcal{U}(t, s) - e^{(t-s)\mathcal{A}(s)})x \right\|_X \\ &\leq \int_s^t C e^{\omega(t-\tau)} (\tau - s)^{\beta-\alpha} e^{\omega(\tau-s)} d\tau \|x\|_X = \frac{C}{1 + \beta - \alpha} e^{\omega(t-s)} (t - s)^{1+\beta-\alpha} \|x\|_X. \end{aligned} \quad (\text{A.11})$$

Thus, we get the estimate for the operator in the norm $\|\cdot\|_X$

$$\left\| \mathcal{U}(t, s) - e^{(t-s)\mathcal{A}(s)} \right\|_X \leq \frac{C}{1 + \beta - \alpha} e^{\omega(t-s)} (t - s)^{1+\beta-\alpha}. \quad (\text{A.12})$$

We denote $\mathcal{U}(T, 0) = \prod_{k=0}^{M-1} \mathcal{U}((k+1)\Delta t, k\Delta t)$. Using the telescoping sum argument, we

obtain

$$\left\| \mathcal{U}(T, 0) - \prod_{k=0}^{M-1} e^{\Delta t \mathcal{A}(k\Delta t)} \right\|_X \quad (\text{A.13})$$

$$= \left\| \sum_{j=0}^{M-1} \prod_{k=j+1}^{M-1} U((k+1)\Delta t, k\Delta t) (\mathcal{U}((j+1)\Delta t, j\Delta t) - e^{\Delta t \mathcal{A}(j\Delta t)}) \prod_{l=0}^{j-1} e^{\Delta t \mathcal{A}(l\Delta t)} \right\|_X \quad (\text{A.14})$$

$$\leq \sum_{j=0}^{M-1} e^{\omega(N-j-1)\Delta t} \frac{C}{1+\beta-\alpha} e^{\omega\Delta t} (\Delta t)^{1+\beta-\alpha} e^{\omega j\Delta t} = \frac{C e^{\omega T}}{1+\beta-\alpha} (\Delta t)^{\beta-\alpha}. \quad (\text{A.15})$$

The statement in (A.7) is proved. \square

For higher order operator splitting methods, in some specific situation the higher order convergence has been proved in [18, 19]. In their works, the assumption Appendix A.7 was largely strengthened, both for the operator $\mathcal{A}(t)$ and initial condition, and the convergence was largely depends on the graph norm $\|v\|_\alpha := \|\mathcal{A}(t)^\alpha v\|_X$. The convergence in norm $\|\cdot\|_X$ is still open and will be our future reasearch plan.

Appendix A.2. Operator splitting methods for solving non-autonomous evolution equations

We study the approximation error of operator splitting methods in solving non-autonomous evolution equations. To be specific, we consider an abstract NCP as follows

$$\begin{cases} \frac{d}{dt}u(t) = (\mathcal{A}(t) + \mathcal{B}(t))u(t), & t \geq s \in \mathbb{R} \\ u(s) = x \in X \end{cases} \quad (\text{A.16})$$

on a Banach space X , where $\mathcal{A}(t)$ and $\mathcal{B}(t)$ are linear operators, $\mathcal{D}(\mathcal{A}(t))$ is independent of t and dense in X , and for each $t \in \mathbb{R}$, $\mathcal{A}(t)$, $\mathcal{B}(t)$ and $\mathcal{A}(t) + \mathcal{B}(t)$ generate strongly continuous semigroups $e^{\cdot\mathcal{A}(t)}$, $e^{\cdot\mathcal{B}(t)}$ and $e^{\cdot(\mathcal{A}(t)+\mathcal{B}(t))}$, respectively. Furthermore, due to the property of evolution equation, solving $u(t)$ and solving $e^{\gamma t}u(t)$ is equivalent, we assume $\|e^{\tau\mathcal{A}(t)}\|_X \leq 1$, $\|e^{\tau\mathcal{B}(t)}\|_X \leq 1$, $\|e^{\tau(\mathcal{A}(t)+\mathcal{B}(t))}\|_X \leq 1$.

We will study the NCP (A.16) based on the perturbation theory. We assume $\mathcal{A}(t)$ is a sectorial operator, which generates an analytical semigroups $e^{\cdot\mathcal{A}(t)}$, and assume $\mathcal{B}(t)$ is bounded, thus $\mathcal{A}(t) + \mathcal{B}(t)$ is also sectorial and generates an analytical semigroups $e^{\cdot(\mathcal{A}(t)+\mathcal{B}(t))}$, where $\mathcal{D}(\mathcal{A}(t) + \mathcal{B}(t)) = \mathcal{D}(\mathcal{A}(t))$. In addition, we assume that the operator $\mathcal{A}(t) + \mathcal{B}(t)$ satisfies assumptions Appendix A.6 and Appendix A.7. Therefore, the corresponding evolution family $\mathcal{U}(t, s)$ solves the NCP problem A.16 and admits an Euler-type approximation, i.e.,

$$\left\| \mathcal{U}(T, 0) - \prod_{k=0}^{M-1} e^{\Delta t (\mathcal{A}+\mathcal{B})(k\Delta t)} \right\|_X \leq C(T) (\Delta t)^{\beta-\alpha}, \quad (\text{A.17})$$

where $T = M\Delta t$, α, β are constants defined in assumptions Appendix A.6 and Appendix A.7.

In the sequel, we analyze the error between $\prod_{k=0}^{M-1} e^{\Delta t (\mathcal{A}+\mathcal{B})(k\Delta t)}$ and $\prod_{k=0}^{M-1} e^{\Delta t \mathcal{A}(k\Delta t)} e^{\Delta t \mathcal{B}(k\Delta t)}$.

First, we list all the assumptions as follows:

- Assumption Appendix A.10.** 1. $\mathcal{A}(t)_{t \geq 0}$ and $\mathcal{B}(t)_{t \geq 0}$ are all linear operators (may be unbounded) on X ,
2. $\mathcal{D}(\mathcal{A}(t))$ are the same for all t and dense in X ,
3. $\|\mathcal{B}(t)\|_X < C$ for all $t \geq 0$,
4. $\mathcal{A}(t)$ satisfies Appendix A.6 and $\mathcal{A}(t) + \mathcal{B}(t)$ satisfies Appendix A.6 and Appendix A.7,
5. $\|e^{\tau \mathcal{A}(t)}\|_X \leq 1, \|e^{\tau \mathcal{B}(t)}\|_X \leq 1, \|e^{\tau(\mathcal{A}(t) + \mathcal{B}(t))}\|_X \leq 1$ for all $\tau \geq 0$.

To obtain a convergence theorem, we need an extra assumption in \mathcal{A} and \mathcal{B} :

Assumption Appendix A.11. For the commutator $[\mathcal{A}(t), \mathcal{B}(t)] = \mathcal{A}(t)\mathcal{B}(t) - \mathcal{B}(t)\mathcal{A}(t)$, we assume that there is a non-negative γ with

$$\|[\mathcal{A}(t), \mathcal{B}(t)]x\|_X \leq c_1 \|\mathcal{A}(t)x\|_X^\gamma \|x\|_X^{1-\gamma}, \quad \forall x \in \mathcal{D}(\mathcal{A}). \quad (\text{A.18})$$

Next is a standard result from [20], and we prove it here.

Theorem Appendix A.12. Suppose assumptions Appendix A.10 and Appendix A.11 are satisfied. We have the following error estimate for the operator splitting method,

$$\|(e^{\tau \mathcal{A}(t)} e^{\tau \mathcal{B}(t)} - e^{\tau(\mathcal{A}(t) + \mathcal{B}(t))})x\|_X \leq C_1 \tau^{2-\gamma} \|x\|_X, \quad \forall x \in X, \quad (\text{A.19})$$

where C_1 depends only on c_1, γ and $\|\mathcal{B}\|_X$.

Proof. We use the freezing coefficient formula and obtain

$$e^{\tau(\mathcal{A}(t) + \mathcal{B}(t))}x = e^{\tau \mathcal{A}(t)}x + \int_0^\tau e^{s \mathcal{A}(t)} \mathcal{B}(t) e^{(\tau-s)(\mathcal{A}(t) + \mathcal{B}(t))} x ds. \quad (\text{A.20})$$

Expressing the term $e^{(\tau-s)(\mathcal{A}(t) + \mathcal{B}(t))}$ using the integral form (A.20), we have

$$e^{\tau(\mathcal{A}(t) + \mathcal{B}(t))}x = e^{\tau \mathcal{A}(t)}x + \int_0^\tau e^{s \mathcal{A}(t)} \mathcal{B}(t) e^{(\tau-s) \mathcal{A}(t)} x ds + R_1 x, \quad (\text{A.21})$$

where

$$R_1 = \int_0^\tau e^{s \mathcal{A}(t)} \mathcal{B}(t) \int_0^{\tau-s} e^{\sigma \mathcal{A}(t)} \mathcal{B}(t) e^{(\tau-s-\sigma)(\mathcal{A}(t) + \mathcal{B}(t))} d\sigma ds. \quad (\text{A.22})$$

We can easily verify that the term R_1 is bounded, i.e., $\|R_1\|_X \leq \frac{1}{2} \tau^2 \|\mathcal{B}(t)\|_X^2$.

On the other hand side, we express the term $e^{\tau \mathcal{B}(t)}$ into exponential series and obtain

$$e^{\tau \mathcal{A}(t)} e^{\tau \mathcal{B}(t)} x = e^{\tau \mathcal{A}(t)} x + \tau e^{\tau \mathcal{A}(t)} \mathcal{B}(t) x + R_2 x, \quad (\text{A.23})$$

where $\|R_2\|_X \leq \frac{1}{2} \tau^2 \|\mathcal{B}(t)\|_X^2$.

Denoted by $f(s) = e^{s \mathcal{A}(t)} \mathcal{B}(t) e^{(\tau-s) \mathcal{A}(t)} x$, we have

$$e^{\tau \mathcal{A}(t)} e^{\tau \mathcal{B}(t)} x - e^{\tau(\mathcal{A}(t) + \mathcal{B}(t))} x = \tau f(\tau) - \int_0^\tau f(s) ds + r = d + r, \quad (\text{A.24})$$

where $d = \tau f(\tau) - \int_0^\tau f(s) ds = \tau^2 \int_0^1 \theta f'(\theta \tau) d\theta$ and $r = R_2 x - R_1 x$.

Since $f'(s) = e^{s\mathcal{A}(t)}[\mathcal{A}(t), \mathcal{B}(t)]e^{(\tau-s)\mathcal{A}(t)}x$, assumption Appendix A.11 implies

$$\|e^{s\mathcal{A}(t)}[\mathcal{A}(t), \mathcal{B}(t)]e^{(\tau-s)\mathcal{A}(t)}x\|_X \leq c_1 \|e^{s\mathcal{A}(t)}\|_X \|\mathcal{A}(t)e^{(\tau-s)\mathcal{A}(t)}x\|_X^\gamma \|e^{(\tau-s)\mathcal{A}(t)}x\|_X^{1-\gamma}. \quad (\text{A.25})$$

By using the property of analytic semigroup Appendix A.8, we know that

$$\|\mathcal{A}(t)e^{(\tau-s)\mathcal{A}(t)}x\|_X \leq C(\tau-s)^{-1}\|x\|_X. \quad (\text{A.26})$$

Thus, we have

$$\begin{aligned} \|d\|_X &= \left\| \tau^2 \int_0^1 \theta f'(\theta\tau) d\theta \right\|_X \leq \tau^2 \int_0^1 C\theta(\tau-\theta\tau)^{-\gamma} d\theta \|v\|_X \\ &= \frac{C}{(1-\gamma)(2-\gamma)} \tau^{2-\gamma} \|v\|_X. \end{aligned} \quad (\text{A.27})$$

Notice that $\|r\|_X \leq \tau^2 \|\mathcal{B}\|_X^2$. We finish the proof. \square

Using the one step estimate obtained in Theorem Appendix A.12, we finally obtain the error estimate for the operator splitting method.

Theorem Appendix A.13. Suppose assumptions Appendix A.10 and Appendix A.11 hold true. We have the following error estimate for the operator splitting method in solving the NCP (A.16).

$$\left\| \prod_{k=0}^{N-1} e^{\Delta t(\mathcal{A}+\mathcal{B})(k\Delta t)} - \prod_{k=0}^{N-1} e^{h\mathcal{A}(k\Delta t)} e^{\Delta t\mathcal{B}(k\Delta t)} \right\|_X \leq C_1(\Delta t)^{1-\gamma}, \quad (\text{A.28})$$

where C_1 is a constant independent of γ .

Proof. We take $t = j\Delta t$ and $s = (j-1)\Delta t$ for $j = 1, \dots, M-1$ in Theorem Appendix A.12, and by using the telescoping sum argument, we obtain that for any $x \in X$,

$$\begin{aligned} & \left\| \prod_{k=0}^{M-1} e^{\Delta t(\mathcal{A}+\mathcal{B})(k\Delta t)} x - \prod_{k=0}^{M-1} e^{\Delta t\mathcal{A}(k\Delta t)} e^{\Delta t\mathcal{B}(k\Delta t)} x \right\|_X \\ &= \left\| \sum_{j=0}^{M-1} \prod_{k=j+1}^{M-1} e^{\Delta t(\mathcal{A}+\mathcal{B})(k\Delta t)} \left(e^{\Delta t(\mathcal{A}+\mathcal{B})(j\Delta t)} - e^{\Delta t\mathcal{A}(j\Delta t)} e^{\Delta t\mathcal{B}(j\Delta t)} \right) \prod_{l=0}^{j-1} e^{\Delta t\mathcal{A}(l\Delta t)} e^{\Delta t\mathcal{B}(l\Delta t)} x \right\|_X \\ &\leq \sum_{j=0}^{M-1} C_1(\Delta t)^{2-\gamma} \left\| \prod_{l=0}^{j-1} e^{\Delta t\mathcal{A}(l\Delta t)} e^{\Delta t\mathcal{B}(l\Delta t)} x \right\|_X \leq \sum_{j=0}^{M-1} C_1(\Delta t)^{2-\gamma} \|x\|_X = C_1(\Delta t)^{1-\gamma} \|x\|_X. \end{aligned} \quad (\text{A.29})$$

Thus, we finish the proof. \square

References

- [1] B. AUDOLY, H. BERESTYCKI, AND Y. POMEAU, *Réaction diffusion en écoulement stationnaire rapide*, Comptes Rendus de l'Académie des Sciences-Series IIB-Mechanics-Physics-Astronomy, 328 (2000), pp. 255–262.
- [2] A. BÁTKAI, P. CSOMÓS, B. FARKAS, AND G. NICKEL, *Operator splitting for non-autonomous evolution equations*, Journal of Functional Analysis, 260 (2011), pp. 2163–2190.
- [3] H. BERESTYCKI, F. HAMEL, AND N. NADIRASHVILI, *The speed of propagation for KPP type problems. I: Periodic framework*, Journal of The European Mathematical Society, 7 (2005), pp. 173–213.
- [4] N. BRUMMELL, F. CATTANEO, AND S. TOBIAS, *Linear and nonlinear dynamo properties of time-dependent ABC flows*, Fluid Dynamics Research, 28 (2001), p. 237.
- [5] C. CHICONE AND Y. LATUSHKIN, *Evolution semigroups in dynamical systems and differential equations*, no. 70, American Mathematical Soc., 1999.
- [6] S. CHILDRESS, *Alpha-effect in flux ropes and sheets*, Physics of the Earth and Planetary Interiors, 20 (1979), pp. 172–180.
- [7] S. CHILDRESS AND A. D. GILBERT, *Stretch, twist, fold: the fast dynamo*, vol. 37, Springer Science & Business Media, 1995.
- [8] P. DEL MORAL, *Feynman-Kac formulae*, in Feynman-Kac Formulae, Springer, 2004, pp. 47–93.
- [9] F. DEN HOLLANDER, *Large deviations*, vol. 14, American Mathematical Soc., 2008.
- [10] T. DOMBRE, U. FRISCH, J. M. GREENE, M. HENON, A. MEHR, AND M. SOWARD, *Chaotic streamlines in the ABC flows*, J. Fluid Mech., 167 (1986), pp. 353–391.
- [11] K. ENGEL AND R. NAGEL, *One-parameter semigroups for linear evolution equations*, vol. 194, Springer Science & Business Media, 1999.
- [12] G. FERRÉ AND G. STOLTZ, *Error estimates on ergodic properties of discretized Feynman–Kac semigroups*, Numerische Mathematik, 143 (2019), pp. 261–313.
- [13] R. FISHER, *The wave of advance of advantageous genes*, Annals of eugenics, 7 (1937), pp. 355–369.
- [14] W. FOULKES, L. MITAS, R. NEEDS, AND G. RAJAGOPAL, *Quantum Monte Carlo simulations of solids*, Reviews of Modern Physics, 73 (2001), p. 33.
- [15] D. GALLOWAY AND M. PROCTOR, *Numerical calculations of fast dynamos in smooth velocity fields with realistic diffusion*, Nature, 356 (1992), p. 691.

- [16] J. GÄRTNER AND M. FREIDLIN, *On the propagation of concentration waves in periodic and random media*, in Doklady Akademii Nauk, vol. 249, Russian Academy of Sciences, 1979, pp. 521–525.
- [17] P. HESS, *Periodic-parabolic boundary value problems and positivity*, Longman, 1991.
- [18] M. HOCHBRUCK AND C. LUBICH, *On Magnus integrators for time-dependent Schrödinger equations*, SIAM Journal on Numerical Analysis, 41 (2003), pp. 945–963.
- [19] M. HOCHBRUCK AND A. OSTERMANN, *Exponential integrators*, Acta Numerica, 19 (2010), pp. 209–286.
- [20] T. JAHNKE AND C. LUBICH, *Error bounds for exponential operator splittings*, BIT Numerical Mathematics, 40 (2000), pp. 735–744.
- [21] T. KATO, *Perturbation theory for linear operators*, vol. 132, Springer Science & Business Media, 2013.
- [22] A. KOLMOGOROV, I. PETROVSKY, AND N. PISKUNOV, *Investigation of the equation of diffusion combined with increasing of the substance and its application to a biology problem*, Bull. Moscow State Univ. Ser. A: Math. Mech, 1 (1937), pp. 1–25.
- [23] J. LYU, Z. WANG, J. XIN, AND Z. ZHANG, *Convergence analysis of stochastic structure-preserving schemes for computing effective diffusivity in random flows*, SIAM Journal on Numerical Analysis, 58 (2020), pp. 3040–3067.
- [24] A. MAJDA AND P. SOUGANIDIS, *Large scale front dynamics for turbulent reaction-diffusion equations with separated velocity scales*, Nonlinearity, 7 (1994), p. 1.
- [25] S. MEYN AND R. L. TWEEDIE, *Stochastic Stability of Markov Chains*, Springer, New York, 1992.
- [26] G. MILSTEIN, G. JOHN, AND S. VLADIMIR, *Transition density estimation for stochastic differential equations via forward-reverse representations*, Bernoulli, 10, pp. 281–312.
- [27] P. D. MORAL AND A. GUIONNET, *On the stability of interacting processes with applications to filtering and genetic algorithms*, Annales De L Institut Henri Poincare-probabilites Et Statistiques, 37 (2001), pp. 155–194.
- [28] P. D. MORAL AND L. MICLO, *Branching and interacting particle systems approximations of Feynman-Kac formulae with applications to non-linear filtering*, in Seminaire de probabilites XXXIV, Springer, 2000, pp. 1–145.
- [29] J. NOLEN, J. ROQUEJOFFRE, L. RYZHIK, AND A. ZLATOŠ, *Existence and non-existence of Fisher-KPP transition fronts*, Archive for Rational Mechanics and Analysis, 203 (2012), pp. 217–246.

- [30] J. NOLEN, M. RUDD, AND J. XIN, *Existence of KPP fronts in spatially-temporally periodic advection and variational principle for propagation speeds*, Dynamics of PDEs, 2 (2005), pp. 1–24.
- [31] J. NOLEN AND J. XIN, *Reaction-diffusion front speeds in spatially-temporally periodic shear flows*, Multiscale Modeling & Simulation, 1 (2003), pp. 554–570.
- [32] ———, *Computing reactive front speeds in random flows by variational principle*, Physica D: Nonlinear Phenomena, 237 (2008), pp. 3172–3177.
- [33] ———, *Asymptotic spreading of KPP reactive fronts in incompressible space-time random flows*, Ann Inst. H. Poincaré, Analyse Non Linéaire, 26 (2009), pp. 815–839.
- [34] A. NOVIKOV AND L. RYZHIK, *Boundary layers and KPP fronts in a cellular flow*, Archive for rational mechanics and analysis, 184 (2007), pp. 23–48.
- [35] A. PAZY, *Semigroups of linear operators and applications to Partial Differential Equations*, vol. 44, Springer Science & Business Media, 2012.
- [36] L. RYZHIK AND A. ZLATOŠ, *KPP pulsating front speed-up by flows*, Communications in Mathematical Sciences, 5 (2007), pp. 575–593.
- [37] R. SCHNAUBELT, *Well-posedness and asymptotic behaviour of non-autonomous linear evolution equations*, in Evolution equations, semigroups and functional analysis, Springer, 2002, pp. 311–338.
- [38] J. SHEN, T. TANG, AND L. WANG, *Spectral methods: algorithms, analysis and applications*, vol. 41, Springer Science & Business Media, 2011.
- [39] L. SHEN, J. XIN, AND A. ZHOU, *Finite element computation of KPP front speeds in 3D cellular and ABC flows*, Mathematical Modelling of Natural Phenomena, 8 (2013), pp. 182–197.
- [40] ———, *Finite element computation of KPP front speeds in cellular and cat’s eye flows*, Journal of Scientific Computing, 55 (2013), pp. 455–470.
- [41] H. STEWART, *Generation of analytic semigroups by strongly elliptic operators*, Transactions of the American Mathematical Society, 199 (1974), pp. 141–162.
- [42] Z. WANG, J. XIN, AND Z. ZHANG, *Sharp uniform in time error estimate on a stochastic structure-preserving Lagrangian method and computation of effective diffusivity in 3D chaotic flows*. To appear in SIAM Multiscale Model. Simul., arXiv:1808.06309.
- [43] ———, *Computing effective diffusivity of chaotic and stochastic flows using structure-preserving schemes*, SIAM Journal on Numerical Analysis, 56 (2018), pp. 2322–2344.
- [44] J. XIN, *Existence of planar flame fronts in convective-diffusive periodic media*, Archive for rational mechanics and analysis, 121 (1992), pp. 205–233.

- [45] —, *Front propagation in heterogeneous media*, SIAM review, 42 (2000), pp. 161–230.
- [46] —, *An introduction to fronts in random media*, vol. 5, Springer Science & Business Media, 2009.
- [47] P. ZU, L. CHEN, AND J. XIN, *A computational study of residual KPP front speeds in time-periodic cellular flows in the small diffusion limit*, Physica D: Nonlinear Phenomena, 311 (2015), pp. 37–44.